Fall 2011

Production and characterization of supported palladium nanoparticles on multiwalled carbon nanotubes by gamma irradiation

Jessika Viviana Rojas Marin

Department:

PRODUCTION AND CHARACTERIZATION OF SUPPORTED PALLADIUM NANOPARTICLES ON MULTIWALLED CARBON NANOTUBES BY GAMMA IRRADIATION

by

JESSIKA ROJAS MARIN

A THESIS

Presented to the Faculty of the Graduate School of the

MISSOURI UNIVERSITY OF SCIENCE AND TECHNOLOGY

In Partial Fulfillment of the Requirements for the Degree

MASTER OF SCIENCE IN NUCLEAR ENGINEERING

2011

Approved by

Carlos H. Castano, Advisor
Manashi Nath
Shoaib Usman
Arvind Kumar

ABSTRACT

Carbon nanotubes are being studied for a variety of applications due to their outstanding mechanical, chemical, electrical, and optical properties that make them interesting in different areas. Nowadays, different methods to modify the structure of the nanotubes are being developed in order to expand the application fields of such materials.

In this work, palladium nanoparticles were directly produced and supported on multi-walled carbon nanotubes (MWCNT) by gamma irradiation. A solution with a 2:1 water-isopropanol ratio was prepared and mixed with palladium chloride as precursor of palladium ions. Radiolysis of water produces certain species that reduce the ions down to a zero-valent state. However, strong oxidizing agents are also produced during irradiation. Hence a scavenger, such as a secondary alcohol, has to be added to the solution in order to balance the reaction. Coalescence of the metal nanoparticles was controlled by the addition of the stabilizer sodium dodecylsulfate (SDS). The size and distribution of the nanoparticles on the nanotubes were studied at different surfactant concentration and radiation doses at a fixed concentration of palladium chloride.

After irradiation, X-ray photoelectron spectroscopy revealed the palladium peaks Pd3d5/2 and Pd3d3/2 at binding energies of 335.9 and 341.1eV, respectively, which are characteristic of metallic palladium (Pd^0), thus confirming the successful reduction of Pd^{+2} to Pd^0. Scanning transmission electron microscopy, and transmission electron microscopy were used for morphological characterization of the nanostructure Pd nanoparticles-CNTs. Nanoparticles obtained for doses between 10 and 40 kGy, ranged in size 5–30 nm. The smaller nanoparticles were obtained at the higher doses and vice versa. Histograms of particle size distributions at different doses are presented.

ACKNOWLEDGMENTS

I would like to express a sincere gratitude to my advisor Dr. Carlos H. Castano for his help, guidance and support during the development of this project. I would also like to thank the members of the committee Dr. Manashi Nath, Dr. Shoaib Usman and Dr. Arvind Kumar for all the help and advice they provided me for the completion of this thesis. I would further like to thank Dr. Stoyan Toshkov from University of Illinois Urbana-Champain, Nuclear Engineering Department who helped me with the sample irradiation.

This thesis could not have been done without funding opportunities from the Nuclear Engineering Department, the Energy Research and Development Center (ERDC), the Materials Research Center (MRC) and the Research Board from Missouri University of Science and Technology.

Most especially, I owe my husband Carlos E. and my family members for the encouragement, enthusiasm and love that enabled me to complete this process. Thanks to my friends in Rolla, my officemate Trahmillia and all those who accompanied me during this time.

TABLE OF CONTENTS

LIST OF ILLUSTRATIONS

Figure Page

LIST OF TABLES

Page

1. INTRODUCTION

Since the discovery of the carbon nanotubes in 1991 by Ijima, they have been proposed for a wide range of potential uses. This material consist of one or up to tens or hundreds of graphene cylinders concentrically aligned with layer spacing around 0.34nm, based on this configuration they are classified as single-walled carbon nanotubes (SWCNT) and multi-walled carbon nanotubes (MWCNT) respectively. Currently, they are being produced by several techniques such as arc discharge, laser ablation and catalytic growth.

Carbon nanotubes have shown outstanding physical, chemical, electrical, optical and mechanical properties that make them attractive for a variety of applications such as, reinforcements for composite materials, electronic devices, field emitters, biological equipments, hydrogen storage and many others [1, 2].

The potential use of nanostructures for effective hydrogen storage has been actively explored during the last decade. Despite previous studies reporting hydrogen capacity in the range from 0.1 to 67 wt%, both reproducibility and reversibility of H_2 storage remain poor. Nowadays, diverse factors in carbon nanostructures are being studied to reach the goal of 6.5% wt in 2010 and 9%wt in 2015 of the Department of Energy (DoE). Some promising results have been reported in this matter [3, 4].

Nanostructures contain impurities (i.e. amorphous carbon, catalyst, hydrocarbons, water, etc.) which can influence hydrogen adsorption. These impurities in the as-produced material change considerably in an uncontrolled manner, leading to large systematic errors. Moreover, a variation in nanostructure type (Multi-walled or single-walled carbon nanotubes), diameter and length may affect hydrogen capacity [5-7].

Several approaches have been made in order to improve the hydrogen storage capacity of the nanotubes by modifying their structure. Purification methods, heat and chemical treatments have been studied. Additionally, CNT doped with transition metals, such as palladium (Pd), vanadium (V), ruthenium (Ru) have been produced showing a significant improvement in hydrogen storage.

Decoration of CNTs with nanoparticles has been carried out by diverse methodologies, including electroless deposition, thermal decomposition, vapor

deposition, chemical reduction in supercritical CO_2 solutions, impregnation and electrodeposition [8, 9].

Ionizing radiation is currently being used as a new alternative to create defects in the surface of the nanotubes and also as a method for production of metallic nanoparticles [10-13]. Gamma (γ) irradiation has shown significant advantages: radiation parameters such as dose and dose rate can be finely controlled, and the reducing agents are generated uniformly in the solution and their strongly reduction potential makes them able to reduce free ions at each encounter [11-12]. Successful attempts have been made to directly deposit metallic nanoparticles such as gold, platinum and ruthenium on carbon nanotubes by gamma irradiation with a homogeneous distribution [13], nonetheless, several factors have to be considered for the process.

In this work, gamma irradiation is used to synthesize and directly deposit palladium nanoparticles on the surface of multi-walled carbon nanotubes. The mechanism and variables that affect the process will be discussed.

2. LITERATURE REVIEW

2.1. GENERALITIES OF CARBON NANOTUBES

The nanotubes may consist of one up to tens and hundreds of concentric graphite sheets wrapped into cylindrical tubes with adjacent shells separation of around 0.34 nm, so called single-walled (SWCNT) and multi-walled carbon nanotubes (MWCNT) respectively. Carbon nanotubes are particularly characterized by their large length to diameter ratio. For SWCNTs, the diameter is in the range of 0.4 to 3 nm and from around 1.4 to at least 100 nm for MWNTs with lengths up to several micrometers. In general, the properties and performance of the nanotubes have shown to be dependent on their geometrical characteristics and configuration [1, 14-15].

Single walled nanotubes are completely described, except for their length, by the chiral vector C. Two equivalent atoms in a planar graphene sheet are chosen and one is used as the origin. The chiral vector C is pointed from the first atom toward the second one as shown in Figure 2.1 and is defined by the relation:

$$C = n\overrightarrow{a_1} + m\overrightarrow{a_2} \quad (1)$$

Where n and m are integers $\overrightarrow{a_1}$ and $\overrightarrow{a_2}$ are the unit cell vectors of the two-dimensional lattice formed by the graphene sheets. Nanotubes are uniquely described by the pair of integers (n,m) and depending on these numbers three types of CNTs are revealed: when n = m, the nanotube is called “armchair” type ($\theta = 0°$); when m = 0, then it is of the “zigzag” type ($\theta = 30°$). Otherwise, when $n \neq m$, it is a “chiral” tube and θ takes a value between 0° and 30°. The value of (n,m) determines the chirality of the nanotube and affects the optical, mechanical and electronic properties. In contrast, multi-walled carbon nanotubes are described by different models which are in good agreement with experiments and in particular with the electron microscopic images [16].

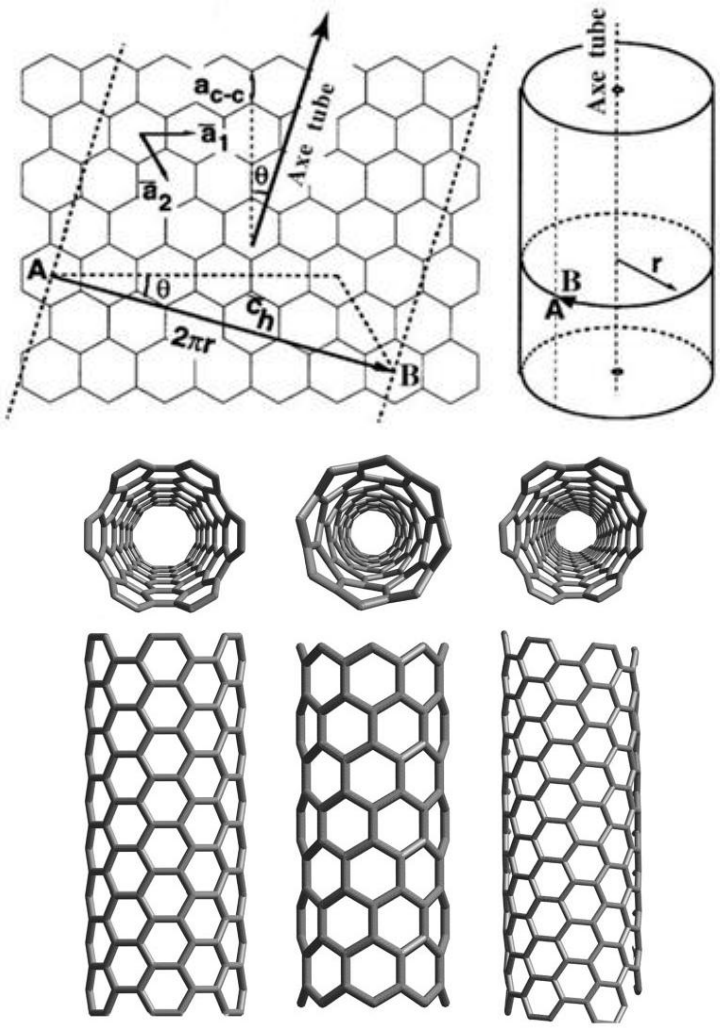

Figure 2.1. Idealized representation of defect-free (n,m) SWNTs with open ends. A) A metallic conducting tube (armchair), B) a zigzag configuration and C) Chiral [16].

Even though carbon nanotubes have a similar structure to a graphite sheet, which is a semiconductor with a zero band gap, they may be either metallic or semiconductors. The electronic properties of the nanotubes are closely related on the direction about which the graphite sheet is wrapped around, a fact that is described by the chiral vector explained above. All armchair SWNTs are conductors, those with n – m = 3k, where k is a nonzero integer, are semiconductors with a small band gap that might vary from 0 to 2eV; and all others are semiconductors with a band gap that inversely depends on the nanotube diameter [14]. MWCNT have similar electronic properties to those of SWCNT which can be explained due to the weak interaction between the cylinders. The electronic

transport in metallic SWCNT and MWCNT occurs ballistically (i.e., without scattering) over long lengths due to the nearly one-dimensional electronic structure, making them able to carry high currents densities up to 10^9 to10^{10} A/cm^2 with essentially no heating or changes in their morphology [14].

In addition to their outstanding electronic properties, carbon nanotubes have shown to have high stiffness and axial strength as a result of the carbon–carbon sp^2 bonding. Practical applications of carbon nanotubes on high mechanical performance systems require the study of the elastic response, the inelastic behavior and buckling, yield strength and fracture. Efforts have been made to investigate these properties from experimental and theoretical points of view, leading to a significant understanding of the behavior of such structures. Although theoretical assumptions and experimental uncertainties led to considerable spread of the mechanical properties, average values have been reported in the literature as summarized in Table 2-1 [1, 14].

Table 2-1. Some mechanical and thermal parameters of carbon nanotubes and its comparison with carbon steel [1, 14].

Material	**Young's modulus (GPa)**	**Tensile strength (GPa)**	**Density (g/cm^3)**
SWCNT	1054.000	150.000	1.4-2.6
MWCNT	1200.000	150.000	
Steel 1%C	208.000	0.400	7.8

Besides the outstanding mechanical and electrical properties of carbon nanotubes, their thermal behavior is also promising. The measured room temperature thermal conductivity for an individual MWNT is around 3000W/m-K which is greater than that of natural diamond and the basal plane of graphite (both 2000 W/m-K), and it is also dependent on temperature [14].

Various applications of nanotubes are currently under investigation, including reinforcements for composite materials, electronic devices, biological equipments, hydrogen storage, and many others. Specifically, several attempts have been made to incorporate carbon nanotubes into polymeric materials in order to develop structural

materials with a considerably increased young modulus and strength. A uniform dispersion of the nanotubes in the matrix is still a challenge, this factor is crucial for achieving an adequate nanotube-matrix adhesion that provides effective stress transfer. With regards to their application on electronics, industrial and academic research activity so far has been mainly focused on using SWNTs and MWNTs as field emission electron sources, for flat panel displays, lamps, gas discharge tubes providing surge protection, and x-ray and microwave generators. As a result of the small radius of curvature of the nanotube tip, when an electric potential is applied between a surface coated with nanotubes and an anode, an extremely high local field is produced and it causes electrons to tunnel from the nanotube tip into the vacuum.

Finally, CNTs seem to be a promising alternative for hydrogen storage, since they are chemically stable and have low mass density. Yet hydrogen storage capacity in nanotubes is still far from being clearly understood [4].

2.1.1. Synthesis and Purification of Carbon Nanotubes. Carbon nanotubes are currently being produced by several methods, namely: arc discharge, laser ablation of carbon, high pressure carbon monoxide (HiPco) and chemical vapor deposition (CVD). The first one involves the generation of an arc discharge between two graphite electrodes placed inside a chamber under a partial pressure of helium or argon (typically 600mbar). During this process the temperature rise up to 6000°C which is enough to cause sublimation of the graphite. The carbon atoms ejected from the solid subsequently head toward colder zones and condensate creating a nanotubes deposit on the cathode. When small amount of transition metals such as Fe, Co, Ni are present in the cathode, SWCNTs are the preferential product. In the absence of those metals, the production of MWCNT is dominant. The second method, a Nd:YAG laser is used to evaporate a solid graphite target into a background gas which is gently flowing through a quartz tube placed in a high temperature oven. The nanotubes then start growing on the water cooled copper collector favored by the suitable temperature gradient created in the furnace. HiPco is used to produce (SWCNT) from the gas-phase reaction of iron carbonyl with high-pressure carbon monoxide gas. Iron pentacarbonyl is used to produce iron nanoparticles that provide a nucleation surface for the transformation of carbon monoxide into carbon during the growth of the nanotubes. Finally, CVD involves the reaction of a carbon

containing gas (such as methane, acetylene ethylene etc.) with a metal catalyst particle such as Co, Ni or Fe or a combination of them. This technique makes possible the synthesis of carbon nanotubes with various shapes and sizes at temperatures below 1000°C. Even though CVD has the advantage of providing a control over the diameter, shell number, growth rate and alignment of CNTs, they have a high defect density due to the low synthesis temperature compared with arc discharge and laser ablation. A schematic representation of the synthesis techniques of carbon nanotubes are shown in Figure 2.2. [1, 18].

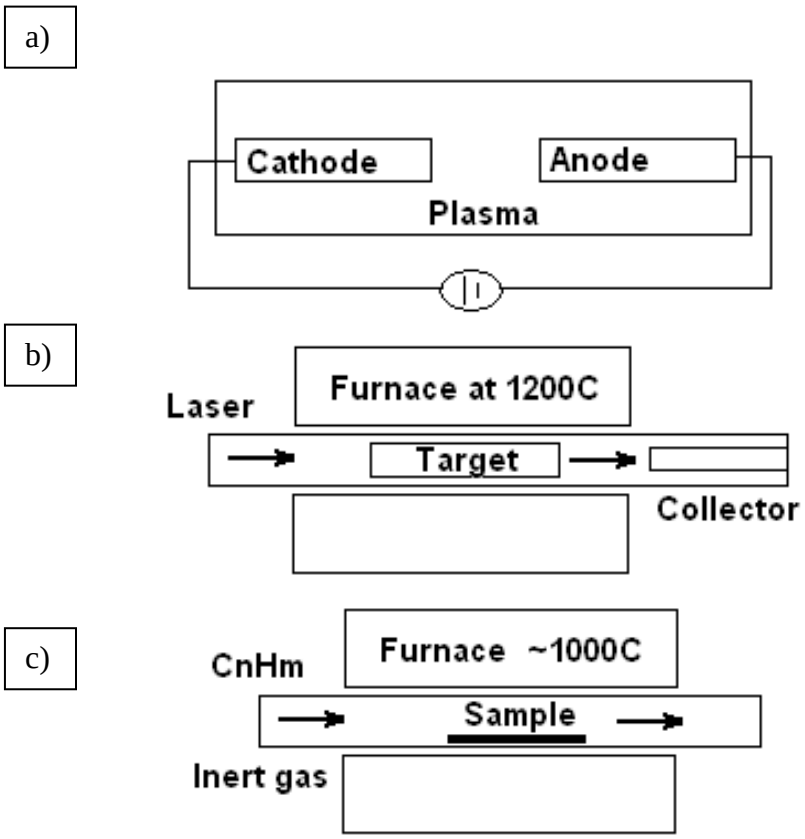

Figure 2.2. Schemes of carbon nanotubes synthesis techniques. a) Arc discharge, b) laser ablation, c) chemical vapor deposition [18].

When Carbon nanotubes are synthesized by any of the methods mentioned above, they contain inevitably carbonaceous impurities (typically carbon nanoparticles,

amorphous carbon and fullerenes) and metal catalyst particles. The presence of these impurities has hindered their industrial applications. Several purification methods have been proposed and can be classified into three main categories: chemical, physical and a combination of both. Chemical methods include gas phase oxidation (using air, O_2, Cl_2, H_2O, etc.), liquid phase oxidation (acid treatment and refluxing, etc.), and electrochemical oxidation. Gas phase purification is characterized by opening the caps of CNTs without greatly increasing sidewall defects or functional groups. Liquid phase oxidation, in addition to the removal of catalyst materials, it introduces functional groups and defects preferentially on CNT side walls, and may cut CNTs into shorter ones with different lengths. The electrochemical oxidation is suitable for purifying CNT arrays without destroying their alignment. Therefore, researchers focus their work on the purification method that best fits on their needs [2]. The use of liquid phase oxidation is commonly found in the literature since it removes simultaneously both amorphous carbon and metal catalyst. Oxidants such as HNO_3, H_2SO_4, H_2O_2 or a mixture of H_2O_2 and HCl, a mixture of H_2SO_4, HNO_3 etc. are preferentially selected. Nitric acid is the most commonly used reagent for CNT purification for its mild oxidation ability. In addition, it is inexpensive and nontoxic, capable of removing metal catalysts and no secondary impurities are introduced [19-23].

On the other hand, the physical method separates is suitable to remove graphitic sheets, carbon nanospheres (CNSs), aggregates or separate CNTs with different diameter/length ratios. This method separates carbon nanotubes from impurities based on their differences in physical size, aspect ratio, gravity, and magnetic properties, etc. Physical separation has the advantage of preventing severe damaging of the nanotubes since it does not involve any chemical oxidation. Nonetheless, it is always complicated, time-consuming and less effective. Lastly, the third kind of purification combines the advantages of physical and chemical purification, and therefore it is a multi-step process. This method can lead to high yield and high-quality CNT products. Owing to the diversity of the as-prepared CNT samples, such as CNT type, CNT morphology and structure, as well as impurity type and morphology, there is a wide variety of purification procedures reported in the literature that provide valuable information to design the appropriate method that best suit for the samples being studied [2, 24].

2.1.2. Functionalization of Carbon Nanotubes. One of the challenges to overcome for several industrial applications of carbon nanotubes is their poor solubility and processability. Poor solubility is mainly caused by the inherent attractive van der Wall's forces between the nanotubes that make them remain stable as tangled aggregates. Introducing various functional groups on the surface of the CNTs is the best method being employed nowadays to improve the dispersion in solution or composite materials. Functionalization methods can be divided in two major groups:

a. Functionalization from inside, which is filling the nanotubes with different nanoparticles. This method uses either the phenomenon of spontaneous penetration, when nanotubes are filled with colloidal suspensions followed by evaporation of the carrier liquid, or the wet chemistry when the nanotubes are filled with some compounds, which react under particular thermal or chemical conditions and produce nanoparticles. These nanoparticles then become trapped inside the nanotubes
b. Chemical functionalization from outside (exohedral). Based in the mechanism of attachment and type of functional groups created, this group can also be divided in three different types: Covalent functionalization by attaching functional groups to the nanotube ends or defects, covalent functionalization through "sidewall functionalization" and noncovalent exohedral functionalization, for example, wrapping nanotubes with polymers [25].

In addition to the ability to remove metallic particles during cleaning process as mentioned before, acid treatments with nitric acid, sulfuric acid, hydrogen peroxide, and others, also create various functional groups on the ends and surface of the nanotubes, such as carboxylic (-COOH), carbonyl (-CH=O), and hydroxylic ($-CH_2OH$). However, acid treatment can also damage the walls of the CNTs and thus produce carbonaceous impurities. In the presence of another strong oxidant like sulfuric acid, concentrated nitric acid can even cut the CNTs into short pieces [19, 26].

2.1.3. Radiochemistry Trends on Carbon Nanotubes Functionalization. Effects of highly energetic ions and electrons on nanostructured materials has been widely studied [27]. A common misconception is that radiation (ions, electrons, gamma rays, etc.) have exclusively detrimental effect on the properties of target materials. Recent experiments show that irradiation can also induce positive effects on nanostructured

systems under specific conditions. Electron or ion beams may serve as tools to synthesize nanoclusters and nanowires, modify in a controllable manner their morphology, and alter their electronic, mechanical, electronic, and magnetic properties. In addition, irradiation of CNT with energetic particles (electrons, ions), can successfully create molecular junctions between the nanotubes (forming cross and Y- shaped structures) and composite materials. The induced defects in the sp2-bonded carbon systems due to focused electron and ions beams is governed by the knock-on displacement of carbon atoms creating vacancies and interstitials in the nanotubes.

Irradiation-induced defects normally increase the reactivity of nanotubes at the surface, thus, functional groups can be attached to graphene and nanotubes in specific areas, which is of special importance for diverse applications. Effects of radiation-induce morphological and structural changes in carbon nanotubes due to focused electron beam as well as immobilization of gold nanoparticles on ion-irradiated regions are shown in Figure 2.3 [27, 28].

Even though the effects of highly energetic particles (electrons, ions) on carbon nanotubes have been studied, limited attention has been given to the effects of gamma irradiation. Recent results have been published on the improvement of both Young modulus and electrical conductivity of gamma irradiated carbon nanotube paper (NT paper), reaching a maximum at a dose of 170 kGy[1]. It has been suggested that highly energetic photons create defects on the nanostructure and that, at a critical defect concentration, the formation of some types of bonds between nanotubes is promoted, affecting the final mechanical and electrical properties. In addition, it has also been observed that the effect of irradiation was much stronger for samples irradiated in air in comparison to those in vacuum.

---

[1] The **absorbed dose** is a measure of the energy deposited in a medium by ionizing radiation per unit mass. It is equal to the energy deposited per unit mass of medium. It may be expressed as Joules per kilogram (J/kg) and represented by the equivalent SI unit, gray (Gy), or rad. $1Gy=100rad=6.254x10^{18}eV/kg$

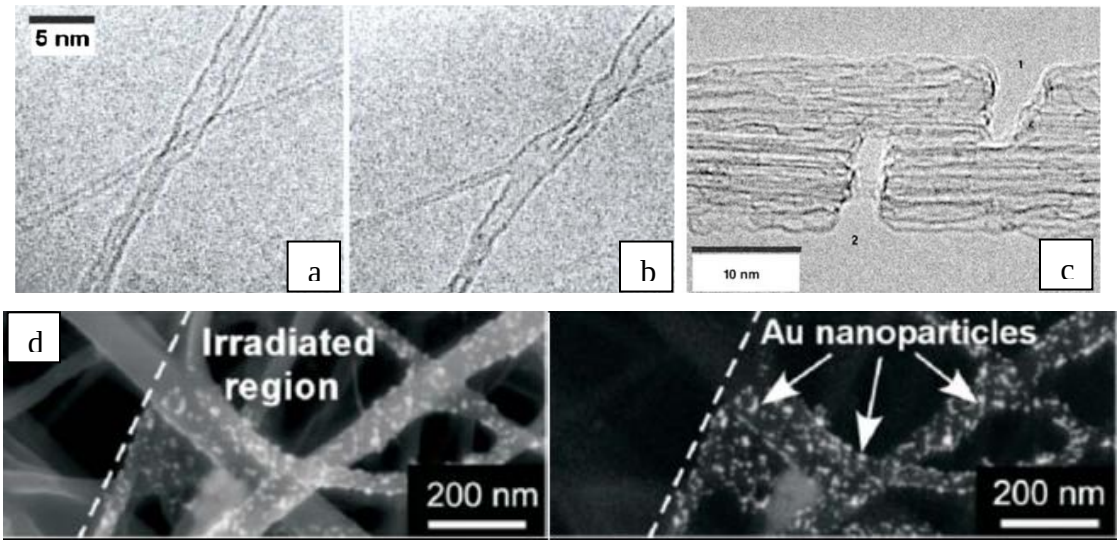

Figure 2.3. Effects of ion- electron irradiation on carbon nanotubes and decoration with nanoparticles. a) SWNTs before electron irradiation, b) 60 s of electron irradiation promotes a molecular connection between the thin and the wide tubes, forming a X junction, c) MWCNT under spatially localized electron irradiation and d)Au nanoparticles on -ion irradiated regions (with 10^{15}–10^{17} cm^{-2} of Ga^{+} ions at 10–30 keV) of MWCNTs [28].

SWNTs irradiated with gamma have been used as a pretreatment for chemical functionalization with thionyl chloride. This process was based on the statement that the concentration of defects is likely to influence the concentration of functional groups attached to the nanotubes [10, 29-30].

Functionalization of MWCNTs with thionyl chloride and decylamine has also been studied after gamma irradiation [31]. The authors report a significant increase of defects on the sidewall of the nanotubes. Furthermore, the concentration of functional groups attached to the nanotubes increases monotonically with increasing irradiation doses in the range of 50 to 250kGy. In addition, more stable dispersions of MWCNTs in organic solvents such as acetone and Tetrahydrofuran TFT were observed, indicating a better solubility of the nanostructure after gamma irradiation [31]. Those previous results indicate that gamma irradiation might be an effective technique to be used as a pretreatment for further functionalization. Further exploration needs to be carried out in this area to better understand the mechanisms and advantages of this technique.

2.2. SYNTHESIS OF METALLIC NANOPARTICLES SUPPORTED ON CARBON NANOTUBES

Decoration of CNTS with nanoparticles has been carried out by diverse methodologies, namely: electroless deposition, thermal decomposition, chemical reduction in supercritical CO_2 solutions, impregnation and electrodeposition. These techniques commonly use noble metal salts as precursors of the nanoparticles, which are obtained by a reduction process [8].

Applications of the electroless deposition methodology is limited to the fact that only metal ions with redox potential higher than that of a reducing agent or the nanotubes can be reduced. Au ($AuCl^-_4$/Au, +1.002 V vs SHE) and Pt ($PtCl_4^{2-}$/Pt, +0.775 vs SHE) nanoparticles have been successfully synthesized by spontaneous reduction if the metal ions by SWCNTs, though Cu^{2+} (Cu- (NO3)2/Cu, +0.340 V vs SHE) or Ag^+ ($Ag(NH3)^{2+}$/Ag, +0.373 V vs SHE) cannot be reduced without the presence of a reducing agent. By using a metal substrate as a support for the nanotubes, ions can be reduced into nanoparticles even if a redox potential lower than the metal ions is used [32].

Thermal decomposition has been used to synthesize nanoparticles of Pd, Pt, Au and Ag, on carbon nanotubes. In this method, carbon nanotubes are dispersed in water or acetone with the addition of a metal salt in a specific weight percent. A subsequent evaporation of the solvent at a temperature around 100°C is carried out and, as a final step, decomposition and reduction of the mixture at temperatures in the range from 300°C to 700°C under H_2 atmosphere. Nanoparticles with sizes between 8 to 20 nm are obtained on the surface of the nanotubes [33].

Nanoparticles such as Pd-Rh have been successfully attached to MWCNTs by chemical reduction in supercritical CO_2 solutions (SC CO_2). Supercritical fluids (SCFs) have a combination of properties such as low viscosity, high diffusivity, near zero surface tension, and strong solvent power for some small molecules that make them applicable in different areas in material science. Although inorganic salts are not generally soluble in SC CO_2, some polar solvents such as ethanol, methanol and acetone, can act as cosolvent to enhance the solubilization of inorganic precursors in supercritical solutions. After reactions, dry and high-purity products are easily obtained by in situ extraction using SC CO_2 as the solvent [34].

As mentioned before, electrodeposition is another method used to produce metal nanoparticles on CNTs. Au, Pt and Pd nanoparticles have been formed on CNTs, by immersing the CNTs in a solution of $HAuCl_4$, K_2PtCl_4, or $(NH_4)_2PdCl_4$ and controlling the potential, the pulse and the concentration of the precursor salt in an electrochemical system.

Many approaches have been developed to support metallic nanoparticles to the nanotubes and, by comparing the different ways, each one has their own advantages and disadvantages. Therefore, it is the potential application what determines which way is preferable each time [8].

Radiochemical methods have also been recently explored as a promising technique to produce and deposit metallic nanoparticles of CNTs. In addition to the ability to create defect sites on the sidewall of carbon nanotubes, gamma irradiation have demonstrated to provide several advantages in the synthesis of nanoparticles, which are: Radiation parameters such as dose and dose rate can be controlled, the reducing agents are generated uniformly in the solution and their strongly reduction potential makes them able to reduce free ions at each encounter and, the controlled reduction of metal ions can be made without excess of reducing agents or producing any undesired oxidation product from the reactant [11, 12]. Successful attempts have been made to directly deposit metallic nanoparticles such as gold, platinum and ruthenium on carbon nanotubes by gamma irradiation with a homogeneous distribution [13, 35]. The method involves exposing the sample in aqueous solution to energetic gamma rays that lead to the formation of hydrated electrons, OH radicals and H atoms. OH radicals, being strongly oxidizing should be converted to reducing radicals by adding a primary or secondary alcohol to the solution. Figure 2.4 depicts the reduction process of the metal ions that takes place during irradiation. As it is shown, the atoms tend to dimerize when they encounter or combine with ions, this happens because the binding energy between atoms or clusters with unreduced ions is stronger that the atom-solvent or atom-ligand energy. [11].

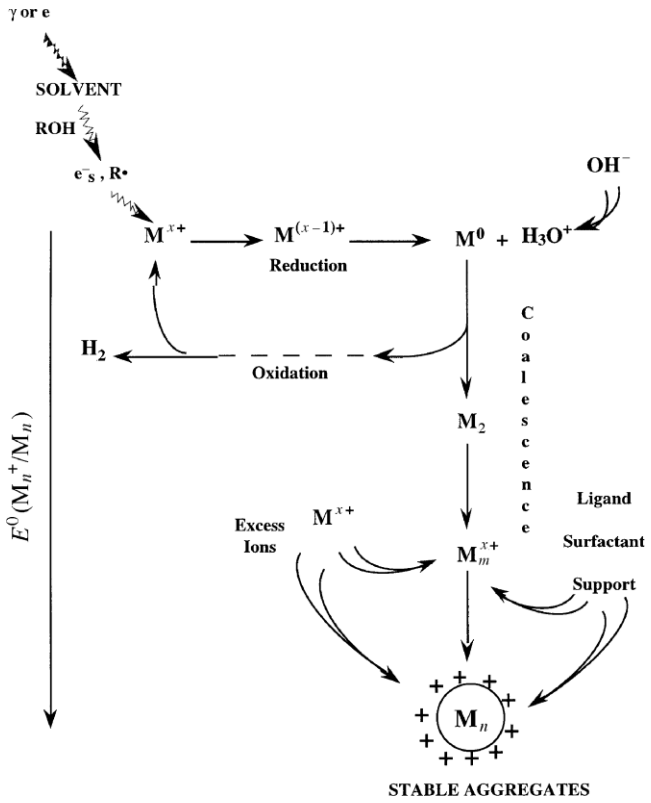

Figure 2.4. Representation of metal ion reduction in aqueous solution by gamma irradiation [11].

In order to limit the coalescence process of the aggregates, polymeric molecules or cluster stabilizers are added to the solution to be irradiated. Functional groups, such as carboxyl groups that have high affinity with the metal, ensure the anchoring of the molecule at the cluster surface, while polymeric chains protect the cluster from coalescing with another at the early stage by electrostatic repulsion or steric hindrance.

When nanoparticles are prepared by irradiation, the stabilizer must be selected in such way that it does not reduce the ions before irradiation. Chemical products such as, poly(vinyl alcohol) (PVA), sodium dodecylsulfate (SDS), sodium poly(vinylsulfate) (PVS), poly(acrylamide) (PAM), poly(N-methylacrylamide) (PNMAM), poly(ethyleneimine) do not affect the electronic state of the ions and fulfill the conditions for stabilizations [11].

Dose rate is also a factor that has to be considered with special attention since it controls the rate at which the ion reduction is occurring. The radiation-induced radicals

are generated randomly in the bulk sample with a quite homogeneous distribution. When the samples are irradiated with a high dose rate (pulse regime), all the reducing species are produced and scavenged in a very short time, which is followed by the cluster formation of atoms separately created. On the other hand, if samples are irradiated with a low dose rate (continuous radiation regime), the production of reducing radicals is slower than the association of ions with atoms, thus the reduction process occurs mostly in the surface of the aggregates. In this case, the reduction of atoms does not contribute to the formation of new clusters but to the growth of the ones already formed [11, 36].

2.3. CARBON NANOTUBES AS PROMISING MEDIUM FOR HYDROGEN STORAGE

Due to our civilization's high energy demand and the environmental impact of fossil fuels, the transition to renewable fuels has become important. Among several possibilities, hydrogen has been positioned as an energy carrier of choice for renewable energy sources due to its high energy per unit mass of 34kcal/g, as summarized in Table 2-2. This value is much smaller when referring to volume-base heating value due to the low density of hydrogen at room temperature and ambient pressure. Efforts to implement hydrogen as a commercially viable transportation fuel alternative to fossil fuels, has been a major focus of research, but safe storage of hydrogen is still an obstacle.

Table 2-2. Heat of combustion of various fuels.

Fuel	Energy (kcal/g)
Hydrogen	34
Petroleum	10.3-8.4
Paraffin	10.3-9.8
Graphite (Coal)	7.8
Castor Oil	9.4
Wood	4.2

Several hydrogen storage systems have been developed so far, liquefaction, compression, metal hydride formation and adsorbents. Liquefaction and compression strategies have the advantage of high storage volume efficiencies, though they have high operating costs. Liquid hydrogen needs to be stored at a maximum temperature of 20K (-253°C), requiring cryogenic systems with superior quality seals. However, up to 40% of the energy content in the hydrogen is lost by this technique. Compressed hydrogen systems have weight and safety concerns related to hydrogen storage at very high pressures. Adsorption-based storage has been typically metal hydrides. Metal hydrides are prepared by reaction between a metal or alloy phase and hydrogen. Typically they exhibit high storage capacities with high dehydriding temperatures or they have low capacities but are easily dehydrided at room temperature. Even though hydrogen in metal hydride is safer than liquefaction and compression, some limitations of metal–hydride systems include inadequate hydrogen-loading, high weight, high alloy costs, and high sensitivity to gaseous impurities [34].

The potential use of nanostructures for effective hydrogen storage has been actively explored during the last decade. Previous studies on hydrogen storage capacity of carbon nanotubes have reported values in the range from 0.1 to 67 wt%. However, the major problematic areas with the use of the carbon materials for hydrogen storage are both reproducibility and reversibility [3]. Although, as prepared carbon nanotubes apparently do not achieve the goal of 6.5wt% of the Department of Energy (DoE), further research is nowadays going on in order to identify the factors that affect the hydrogen storage capacity of carbon nanostructures. Some promising results have been reported in this matter [4, 5]. As a result of manufacturing processes, impurities in the nanostructures, such as amorphous carbon, catalyst materials, hydrocarbons, water, can influence hydrogen adsorption. These impurities in the as-produced material change considerably in an uncontrolled manner leading to large systematic errors. Furthermore, a variation in nanostructure type (multi-walled or single-walled carbon nanotubes), diameter and length may affect hydrogen capacity [4-6].

Hydrogen has two possible ways to be stored in carbon nanotubes: interstitial sites and inside the tubes. During gas loading, the physisorption of hydrogen molecules may be limited by steric factors representing impurities blocking the access to the internal

storage space of nanostructures. Opening cap at the ends and creating defects in the surface of the nanotubes can serve as a path for hydrogen to easily enter into the nanotubes. Also cutting the nanotubes in shorter pieces may help the diffusion process [39]. Acid treatments to nanotubes are frequently performed to promote those changes, however, systematic experimental procedures and intercomparisons among the different treatments are still in progress. On the other hand, purification, functionalization and heat treatment processes need to be fully understood to be able to control the experimental parameters in order to enhance the storage capacity [40, 41].

Another approach to increase the hydrogen storage capacity of the nanotubes is by adorning them with transition metals such as Pd, V, Pt and Ti. CNTs doped with metal nanoparticles have indicated in the past an increase in hydrogen storage capacity when compared with the pristine samples. The increased hydrogen storage capacity of transition metal-doped carbon nanostructures is attributed to the initial hydrogen adsorption by metal nanoparticles which subsequently dissociate the hydrogen molecules and spill them over to carbon nanotubes [38, 42, 43]. Table 2-3 shows the hydrogen storage capacity of carbon nanotubes decorated with metallic nanoparticles such as palladium and vanadium with different treatments and deposition methods.

Table 2-3. Hydrogen storage capacity of carbon nanotubes decorated with metallic nanoparticles.

System	Deposition method	Pressure (MPa)	Temperature (K)	%wt H_2
MWCNT-Pd	HCl-HNO_3 treatment Refluxing with hydrogen gas	6.5	77 300	0.37 [42] 0.125
MWCNT-V	HCl-HNO_3 treatment Vapor deposition	6.5	77 300	0.4 [42] 0.1
MWCNT-Pd	Electroless deposition	2	300	0.66 [43]
MWCNT-V	impregnation		300	0.69 [43]

Table 2-3. Hydrogen storage capacity of carbon nanotubes decorated with metallic nanoparticles (cont).

System	Deposition method	Pressure (MPa)	Temperature (K)	%wt H_2
Pd/CNTs	No treatment	2.3	298	0.18 [44]
Pd/CNTs	No treatment	10.7	300	0.6 [45]
Pd/CNTs	2 hr plasma etching-Impregnation	10.7	300	1 [45]
Pd/CNTs	4 hr plasma etching Impregnation	10.7	300	1.4 [45]

3. RESEARCH OBJECTIVES

The objective of this research is to produce palladium nanoparticles supported on multi-walled carbon nanotubes using gamma irradiation. The addition of metallic nanoparticles on carbon nanotubes has been studied for several applications in catalysis, nanoelectronics, optics, nanobiotechnology etc. Palladium is of primary importance in hydrogen storage since it has shown to increase the hydrogen storage capacity of the carbon nanotubes.

Several methods have been reported to produce and attach metallic nanoparticles to the surface of the carbon nanotubes, such as electroless deposition, thermal decomposition, vapor deposition, electrodeposition and some others. Gamma irradiation is to be studied as an alternative way to produce metallic nanoparticles and support them on carbon nanotubes. This method provides several advantages over others, including the fact that the amount of radicals created due to water radiolysis is homogeneously dispersed in the sample and it can be controlled by changing the dose.

The samples are prepared using palladium chloride ($PdCl_2$) as a precursor of metal ions and in a solution of water-isopropanol. Two factors are controlled during the process in order to identify their effect on the particle size and distribution on the nanotubes, the amount of stabilizer added to the solution and the radiation dose, which will lead to an optimization of the technique. The nanostructure Pd nanoparticles-MWCNT are to be characterized qualitatively by scanning transmission electron microscopy (STEM), transmission electron microscopy (TEM) in order to determine the dispersion and size of the metal nanoparticles. Additionally, the interaction of palladium and the carbon nanotubes is to be studied using X ray photoelectron spectroscopy (XPS).

4. MATERIALS AND METHODS

4.1. MATERIALS DESCRIPTION

Commercially available multi-walled carbon nanotubes (MWCNT) were received from Alfa Aesar. These nanotubes are synthesized by CVD method and they were supplied with a final purity of 95%. The outside diameter of the CNTs is in the range from 3 to 20 nm, internal diameter from 1 to 3 nm and lengths in the interval of 0.1 to 10 micrometers. For further purification and sidewall functionalization, 65 % v/v commercial nitric acid (HNO_3) was obtained from ACROS Organics. Additionally, palladium chloride ($PdCl_2$) was selected as metal precursor for palladium nanoparticles, sodium dodecyl sulfate (SDS, ($C_{12}H_{25}SO_4Na$) as suspension stabilizer and Isopropyl alcohol 99% as chemical scavenger. These chemical components were also purchased from Alfa Aesar. Deionized water was used throughout the sample preparation and washing procedures.

4.2. CHEMICAL TREATMENT WITH NITRIC ACID

In order to remove impurities present in the carbon nanotubes, such as carbonaceous material and catalyst metal particles, an acid treatment was carried out. In this procedure, 100mg of MWCNT were placed in a round bottom glass flask with 10ml of concentrated nitric acid 15.6 M (65 % v/v). The solution was sonicated for 30 minutes in order to eliminate bundles and obtain a better dispersion of the carbon nanotubes. Once this process is done, the flask was assembled to a reflux condenser and placed over a heating mantle and a magnetic stirrer. The purpose of the stirrer is basically to keep a good dispersion of the nanotubes throughout the chemical treatment. The temperature remained between 60°C and 80°C during a period of time selected for the reaction. The experimental set-up is shown in Figure 4.1.

Once the chemical reaction reached a period of time of 6 hours, half of the liquid was taken out from the flask and the other part continued the treatment until reaching 9 hours. Right after the 6h and 9h of nitric acid treatment had finished for each sample, they were mixed, separately, with abundant deionized water and centrifugated for 20min to accelerate the settlement of the nanotubes and avoid further damaging due to the acid.

The supernatant was carefully removed after every centrifugation and the remaining solid (carbon nanotubes) was rinsed again with water and gently shaken to ensure a good mixing before placing the tubes in the centrifuge. This step was repeated several times in order to remove the excess of nitric acid until reaching a pH around 5. During this step up to 10% of carbon nanotubes was lost due to the high solubility after the chemical treatment. As a final step, the samples were dried in an oven at approximately 40°C.

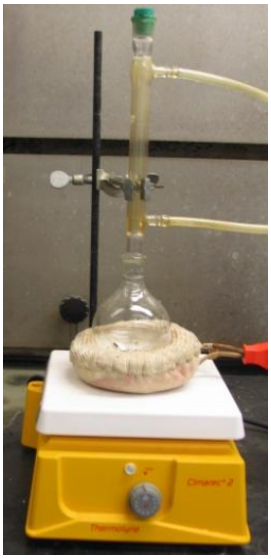

Figure 4.1. Set-up for nitric acid treatment of MWCNT.

4.3. SYNTHESIS OF PALLADIUM ADORNED CARBON NANOTUBES (CNTs)

Small scale batches containing 1ml of an aqueous dispersion of palladium chloride, MWCNT and water-isopropanol were prepared. Initially, 12 mg of $PdCl_2$ and 12mg of carbon nanotubes were added to 12ml of deionized water-isopropanol mixture (2:1 v/v) and sonicated for approximately 30 minutes. This results in a concentration of palladium ions in solution and isopropanol of $5.6x10^{-3}$ mol/dm^3 and $4.4mol/dm^3$ respectively. This dispersion was distributed in sample vials containing various amounts of SDS resulting in concentration of 14.6mg/ml (0.05M), 20.6 mg/ml (0.07M) and 29.7mg/ml (0.1M). Four samples of each SDS concentration were prepared. The specimens were placed in an ultrasonic bath for 30 minutes with the aim of breaking the

bundles of nanotubes and obtain a homogeneous distribution of the different chemical components. Finally, the glass vials containing the dispersions were degassed with argon to remove oxygen. The samples were transported to the University of Illinois, Urbana-Champaign Nuclear Radiation Facility, and subjected to gamma irradiation. A Gammacell 220 Excell Cobalt irradiator [MDS Nordion 447, Ontario, Canada, K2K 1 × 8], shown in Figure 4.2 with a cylindrical irradiation chamber of 203 mm (high) by 152 mm (diameter) was used for this purpose. Sets of three samples with the different SDS concentrations were irradiated at four doses of 10, 20, 30 and 40 kGy with a dose rate of 10kGy/hr (10 kGy/hr = 1Mrad/hr). After irradiation, the dispersions were washed with deionized water several times to remove the excess of surfactant and finally stored in acetone.

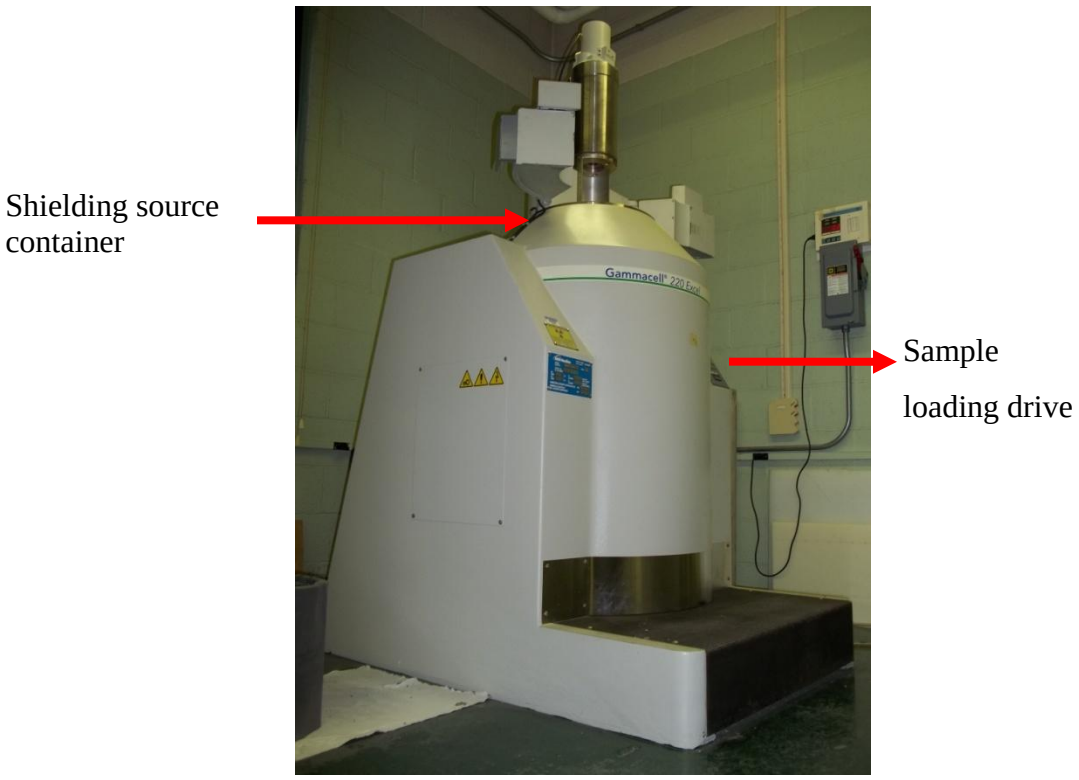

Figure 4.2 The external features of Gammacell 220 Excel.

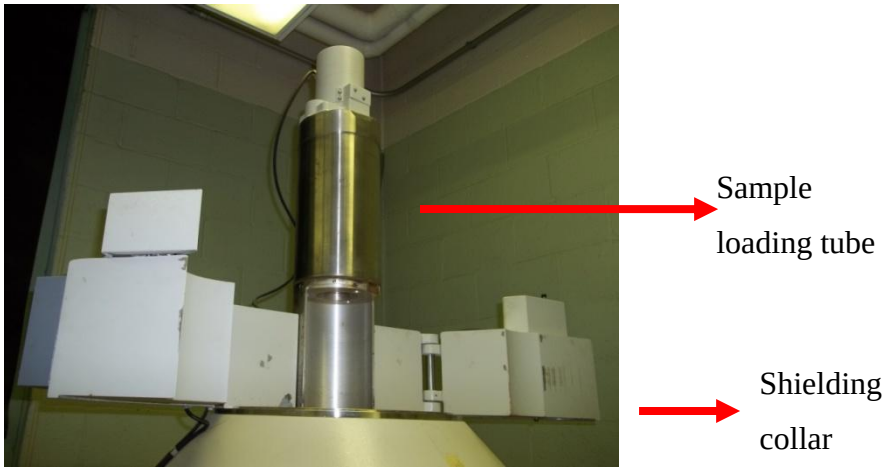

Figure 4.2. The external features of Gammacell 220 Excel (cont).

4.4. CHARACTERIZATION TECHNIQUES

Given the nanometric scale nature of the carbon nanotubes, only a reduced number of characterization techniques can be used. Moreover, only few are able to characterize individual carbon nanotubes and nanoparticles such as scanning tunneling microscope (STM), transmission electron microscopy (TEM) and scanning transmission electron microscopy (STEM). On the other hand, techniques such as X-ray photoelectron spectroscopy (XPS), infrared spectroscopy (FTIR) Energy dispersive X-ray spectroscopy (EDS) are helpful to characterize the chemical structure and qualitative chemical composition. Due to the advantages and limitations of the techniques mentioned above, they cannot be used separately but in a complementary way in order to obtain a proper characterization of the nanotubes.

In this work, TEM, EDS, XPS, Raman spectroscopy, and FTIR spectroscopy were used to characterize the nanotubes decorated with Pd nanoparticles. The uses of each technique, information that can be obtained and sample preparation are explained in detail in this section.

4.4.1. Raman Spectroscopy. This technique is one of the most widely used for analysis of structural changes in carbon nanotubes that provides vibrational properties and electronic structures. Raman scattering refers to the inelastic scattering of light. This phenomenon takes place when a photon with a certain wavelength alters a molecule and

interacts with the electron cloud and the bonds a molecule. As a result, a photon excites the molecule from the ground state. Afterwards, the molecule returns to a different rotational or vibrational state by emitting a photon. The difference in energy between the original and the new state causes a shift in the frequency of the emitted photon up or down from the excitation photon wavelength. This shift gives valuable information about vibrational, rotational and other low frequency transitions in molecules.

Several peaks can be identified in a Raman spectrum obtained from carbon nanotubes. The radial breathing mode (RBM) is usually the strongest peak characteristic of SWCNT, where all the carbon atoms are moving in-phase in the radial direction. This peak is not observable in multiwalled carbon nanotubes. Another distinguishable feature is the G-band (or tangential mode) which is an intrinsic feature of carbon nanotubes closely related to vibrations in all sp2 carbon materials. In addition, the D-band (disorder band) in graphite involves scattering from a defect which breaks the basic symmetry of the graphene sheet, it is observed in sp2 carbons containing porous, impurities or other symmetry-breaking.

For sample preparation, around 30mg of solid dried MWCNTs were placed in a glass microscope slide and finally located inside the Raman spectrometer. A LabRam Aramis equipment available on campus (Material Science and Engineering- Ceramic Engineering) equipped with a HeNe (Helium-Neon) laser with wavelength of 632.8nm was used for analysis, as shown in Figure 4.3.

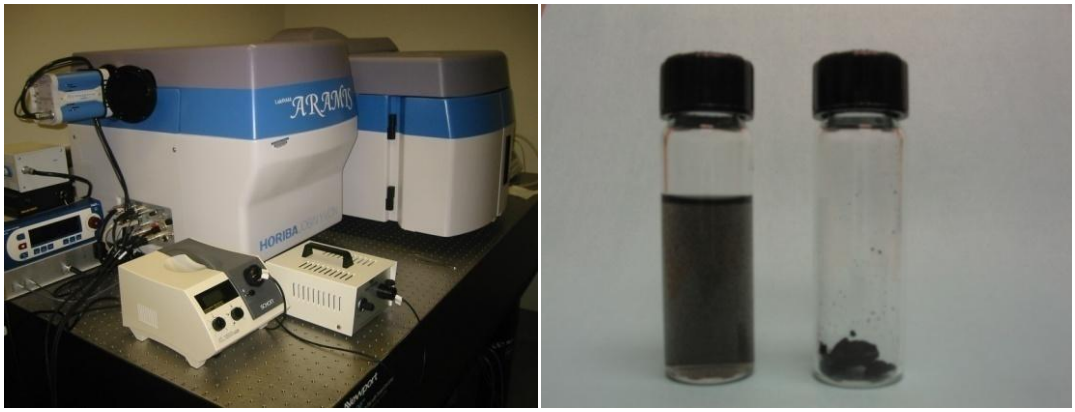

Figure 4.3. LabRam Aramis Raman spectrometer equipped with HeNe (Helium-Neon) laser.

4.4.2. Fourier Transform Infrared Spectroscopy (FTIR). This technique is widely used in materials chemistry. It is basically the absorption measurement of different IR frequencies by a sample placed in the path of an IR beam. The main target of using IR spectroscopic analysis is to determine the chemical functional groups in the sample. Due to the differences of chemical of the diverse functional groups, they absorb characteristic frequencies of IR radiation, thus each absorption peak in the spectrum correspond to a specific group. This technique provides a fingerprint of the material being analyzed and it is complementary of Raman spectroscopy. A FTIR spectrometer NICOLET NEXUS 470 available in campus in Chemistry department was used for the analysis as shown in Figure 4.4.

Figure 4.4. FTIR spectrometer NICOLET NEXUS 470.

The samples were prepared by mixing a small amount of nanotubes and mixing them with dry potassium bromide (KBr), the ratio was approximately 1: 10 in order to get a good transparence. Followed this, the mixture was grinded together in a mortar with pestle. Finally, the mixture was loaded into a pneumatic press by putting a small amount into the press cell. 15000PSI of pressure was used to compress the sample. The final pellet was located in the sample holder for analysis.

4.4.3. Transmission Electron Microscopy (TEM) and Scanning Transmission Electron Microscopy (STEM). The resolution of a traditional optical microscopes is directly dependent on the light wavelength, thus limiting their resolutions to around 0.2 micrometers. The use of electron beams instead, whose wavelength is smaller by far, have made possible the development of high resolution microscopes such as scanning electron microscopes (SEM) and transmission electron microscopes (TEM). This last technique has been very useful in nanomaterials so it has a resolution up to 0.5Å. A TEM consist basically of an electron source that is focused by using a precise arrangement of apertures and electromagnetic lenses. When the beam passes through a thin (less than 100nm) specimen they are forward scattered to certain angles that depend on the size and density of different elements that conforms the sample. Heavy atoms, such palladium, will scatter the electrons from the beam to higher angles as compared to carbon. As a result, high atomic number materials will appear either darker or brighter when using bright field (BFD) or dark field detector (DFD) respectively.

A HELIOS Nano Lab 600 dual beam equipped with a scanning transmission electron microscope (STEM) was used to characterize the carbon nanotubes decorated with palladium nanoparticles. In STEM mode the beam is moving through the samples and scanning the surface. The images were obtained at the recommended conditions of 30 kV of accelerating voltage and a current of 43pA. Even though the voltage is not as higher as it is in conventional TEM (up to 200kV), it is high enough to detect the metallic nanoparticles on the carbon nanotubes and carry out an initial characterization.

A transmission electron microscope (TEM) TECNAI F20 was also used for a more detailed characterization of the most representative samples. Since a TEM provides high resolution, it is possible to study the size and distribution of the nanoparticles. In addition, STEM mode was also set in order to carry out energy dispersive X-ray spectroscopy (EDS) point analysis of the nanoparticles. The equipments used for this process are shown in Figure 4.5.

Figure 4.5. Transmission electron microscope (TEM) TECNAI F20 and Helios Nanolab 600 FIB/SEM. TEM left side and FIB right side, both equipments available at the Material research center (MRC) on the campus of Missouri S&T.

With the aim of preparing the samples for STEM and TEM analysis a small amount of the carbon nanotubes was placed in a glass vial and diluted in acetone. The dispersion was sonicated during 30 min in order to minimize the agglomerates and obtain a homogeneous distribution of the nanotubes in the liquid. Several drops of the dispersion were then placed onto a 300 mesh TEM carbon coated copper grid and let the acetone evaporate as shown in Figure 4.6. Acetone was used for this process due to its low surface tension that keeps the nanotubes well distributed all over the sample and its high volatility at room temperature. The layer of carbon on the grid is thin enough so that is essentially electron transparent, but thick enough to support the individual CNTs on the surface.

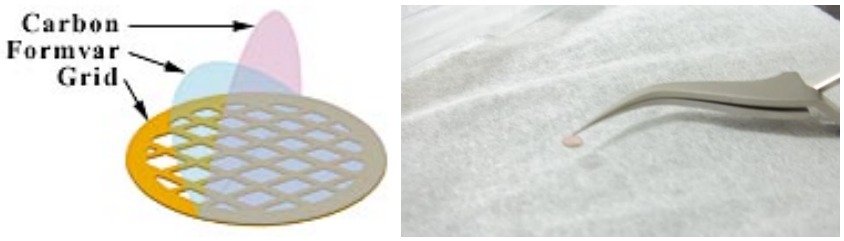

Figure 4.6. Schematic steps for sample preparation for STEM/TEM.

4.4.4. X-ray Photoelectron Spectroscopy (XPS). XPS technique can give information about the surface chemical structure of the material being analyzed. During the analysis the sample is irradiated with energetic X-rays and the kinetic energy of the electrons that are ejected from the sample is simultaneously measured. This measurement is directly related with the binding energy of the electron being detected that is characteristic of the each element present in the sample. In addition, it allows the identification of the electronic configuration of the electrons in the atoms.

The samples were prepared by dispersing a small amount of nanotubes decorated with palladium nanoparticles in acetone and sonicating them for 30 minutes to obtain good dispersion. A drop of such dispersion was then deposited on the surface of a silicon substrate and let to dry. This step was repeated until a thin layer of nanotubes fully covering the substrate was observed. Figure 4.7 shows a photoelectron spectrometer (XPS) KRATOS AXIS 165 X-ray that uses either a magnesium or monochromated aluminum. This equipment, located at the materials characterization center (MRC), was used to identify the electronic states of carbon and palladium in the samples after irradiation.

Figure 4.7. Left side: KRATOS AXIS 165 X-ray Photoelectron Spectrometer (XPS) located at the materials research center (MRC) on campus.

5. RESULTS AND DISCUSSION

5.1. PRELIMINARY CHARACTERIZATION

Morphological characterization was carried out with an STEM and images were obtained for the MWCNTs before and after chemical treatment. Figure 5.1 shows the carbon nanotubes before any treatment; showing amorphous carbon and some metallic particles around the sample. The presence of those particles is residues of the catalyst used for the production of the nanotubes.

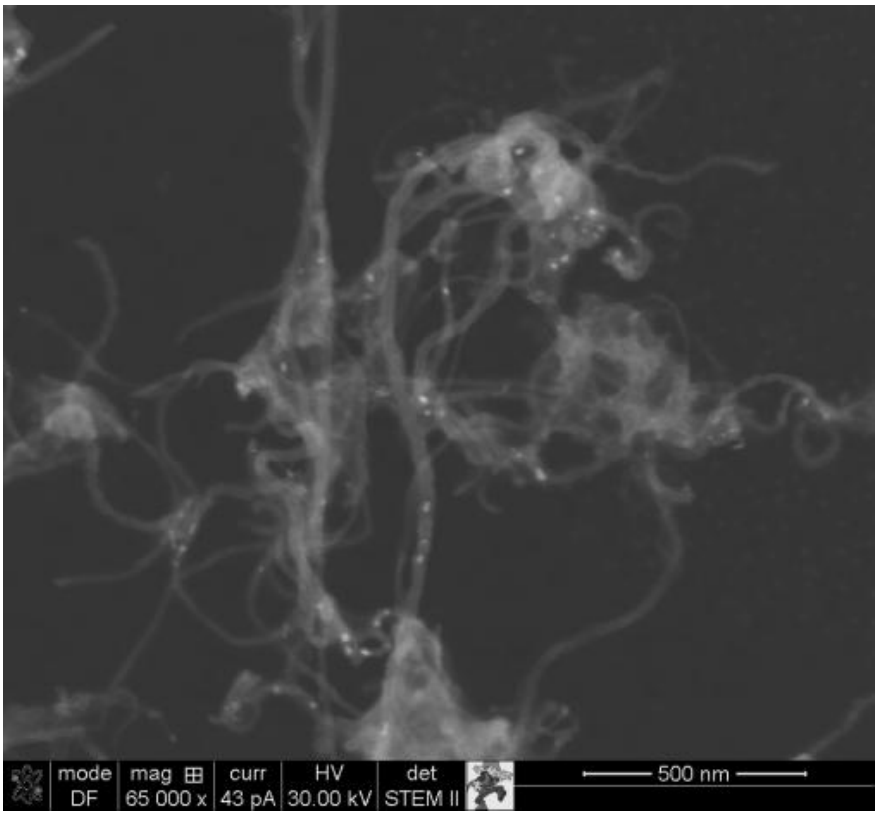

Figure 5.1. Multiwalled carbon nanotubes 95% purity before chemical treatment.

The chemical nature of the metallic nanoparticles was detected with EDS. The spectrum shown in Figure 5.2 verifies the presence of metallic elements such as

aluminum (Al), copper (Cu), nickel (Ni), titanium (Ti), and silicon (Si). Al, Cu, Ni and Si peaks might be due to the interaction of the electrons with the grid and detector.

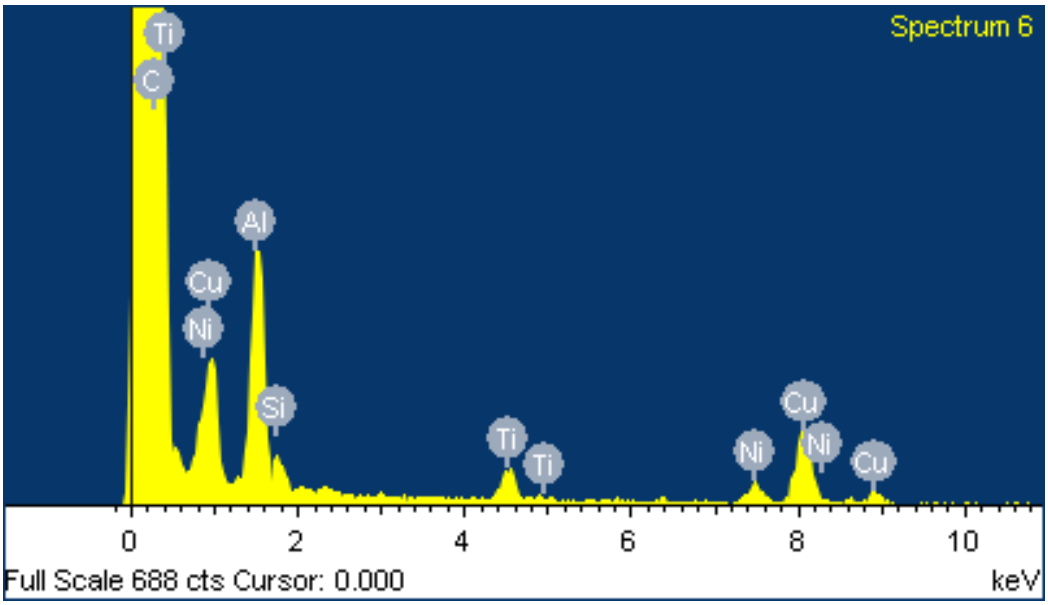

Figure 5.2. EDS spectrum of as received MWCNT.

Morphological changes of carbon nanotubes after nitric acid treatment for periods of time of 3 and 6 hours are shown in Figure 5.3. After 6 hours acid treatment, the reduction of the metallic particles and carbonaceous impurities is remarkable as observed in Figure 5.3 a). Finally, after 9 hours of treatment the oxidation process that takes place in the reaction begins to destroy the nanotubes. It can be noticed that the ends of the CNTs become amorphous material, this feature is highlighted in Figure 5.3 b) with ovals enclosing some representative regions.

Acidic treatments purification of carbon nanotubes is important for many applications. Nitric acid treatment of carbon nanotubes leads not only to the removal of amorphous carbon and catalyst material but also, to the formation of defects on the ends and the carbon nanotubes walls.

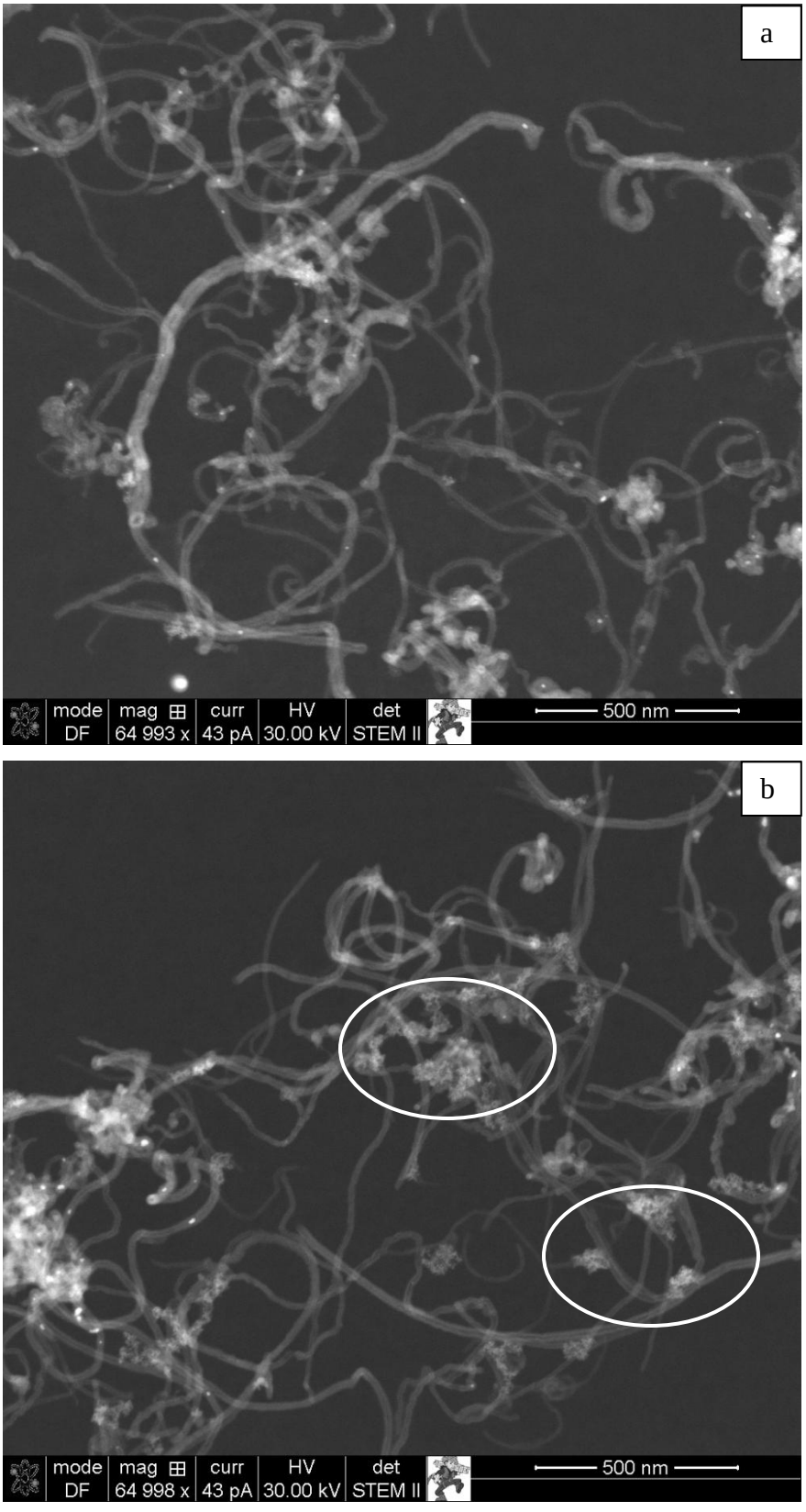

Figure 5.3 Multiwalled carbon nanotubes after chemical treatment with nitric acid 15.6M. a) During 6 hours, b) during 9 hours.

FTIR spectra of as received and acid treated MWCNTS are shown in Figure 5.4. Several features are identified, including an intense peak in the spectrum observed at a wavenumber 3441cm^{-1} attributed to the stretching vibrations of isolated surface–OH moieties and/or –OH in carboxyl groups (O=C−OH and C−OH) and in sorbed water. However, it is also noticed that this peak shifts in the wavenumber to lower values after the chemical treatment, indicating the presence of strong hydrogen bonds between –OH groups. Secondly, a group of peaks in the range between 1750–1550cm^{-1} which can be assigned to C=O groups in different environments and to C=C in aromatic rings. Lastly, the bands in the range of 1300–950cm^{-1} confirm the presence of C–O bonds in various chemical surroundings. A band observed at a wavenumber around 1550cm^{-1} in the as-prepared and treated MWCNTs is most probably due to aromatic and unsaturated structure of C= C bonds. As a result of functionalization, the intensity increase of the peaks in the 2800-3050 cm^{-1} region are characteristic of C-H stretch modes of H−C=O in the carboxyl group, additionally the C-O bands characteristic of carboxyl functional groups (–COOH) and of ketone/quinone are observed at 1711 and 1638cm^{-1}, respectively. A schematic representation of the carboxilation process due to acid treatment is presented in Figure 5.5.

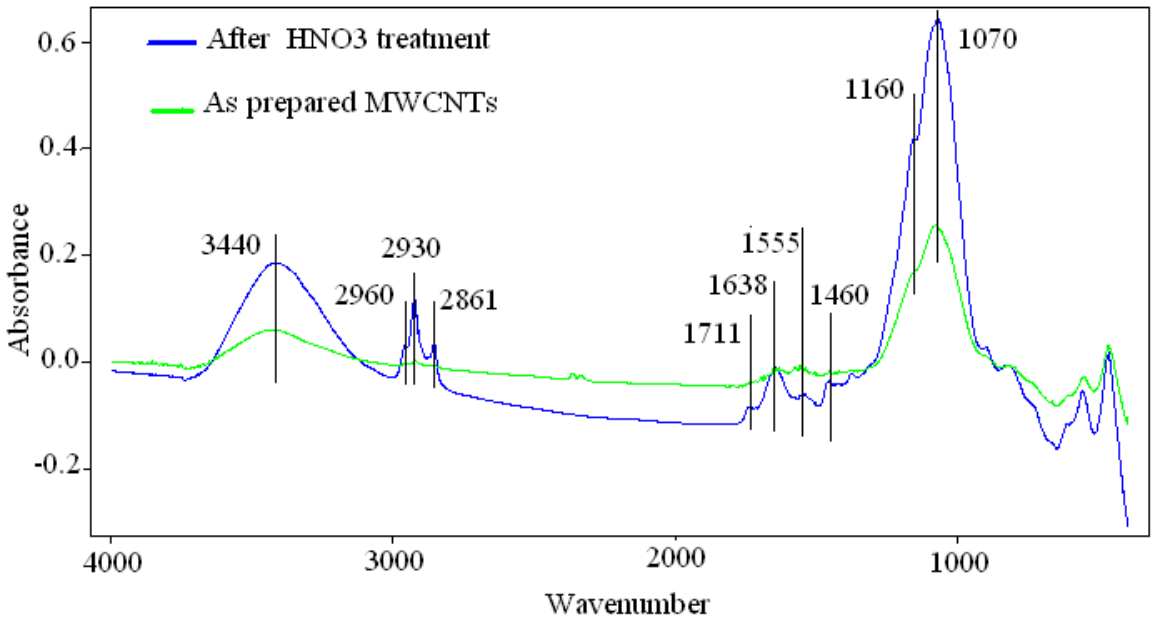

Figure 5.4. FTIR spectra of MWCNTs before and after nitric acid treatment.

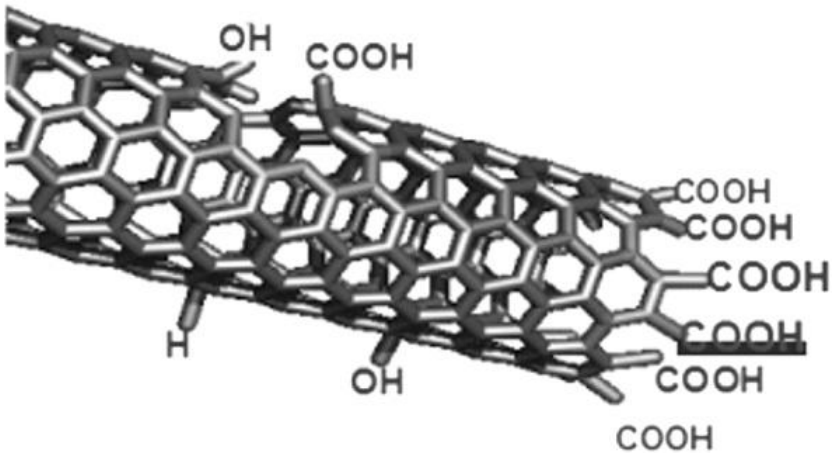

Figure 5.5. Scheme of carboxilation on MWCNTs during the oxidation process [46].

Raman spectra for MWCNTs before and after nitric acid treatment are presented in Figure 5.6. There are three remarkable peaks, D, G and D* bands. D band usually appears in the range 1250-1350cm^{-1} which was observed in this case at 1325 cm^{-1}. The frequency at which this line shows up is laser energy dependant and does not correspond to a vibrational mode in the center of the Brillouin Zone; D line is the result of a double resonant process where an electron is scattered elastically by a structural defects. G band is characteristic for most of the carbonaceous materials and corresponds to carbon-carbon bonds elongation. This band appears in the range 1500-1600cm^{-1}. Finally, D* band which is the second harmonic of D band emerges in the range 2500-2700 cm^{-1}.

Table 5-1 shows the intensity and position in the Raman spectrum of G and D bands of MWCNT treated with HNO_3 for different time lengths. The IG/ID ratio of as prepared MWCNT sample was 0.68; this indicated a high quantity of structural defects in the MWCNT graphitic structure which provided a lot of active sites. The intensity ratio vs. treatment time is additionally shown in Figure 5.6b). There, it is possible to identify a decrease in the IG/ID ratio, this aspect is due not only to the increment of the density of structural defect but also it might be associated with the formation of carbonaceous material produced by shortening or thinning the MWCNT. Moreover, the relationship between the density of defects and the intensity of the D band is not straightforward

because several factors might affect it, such us the amount of carbonaceous species, polarization and electronic properties of the sample [18].

The defects density also plays an important role in the solubility of the carbon nanotubes in different solvents, which is essential for subsequent functionalization process. It was noticed after the chemical treatment a considerable difficulty to physically separate the carbon nanotubes from the nitric acid, then, a large amount of sample was lost in solution with the acid. Other authors have reported levels of solubility of 10mg/ml for multi-walled carbon nanotubes in deionized water after treatment with nitric acid 60%v/v during 9-12h and no changes in the amorphous content compared with the initial sample [19].

Hydrogen storage capacity of treated nanotubes is presented in Appendix A where a brief discussion of the improvement in the hydrogen storage capacity is made.

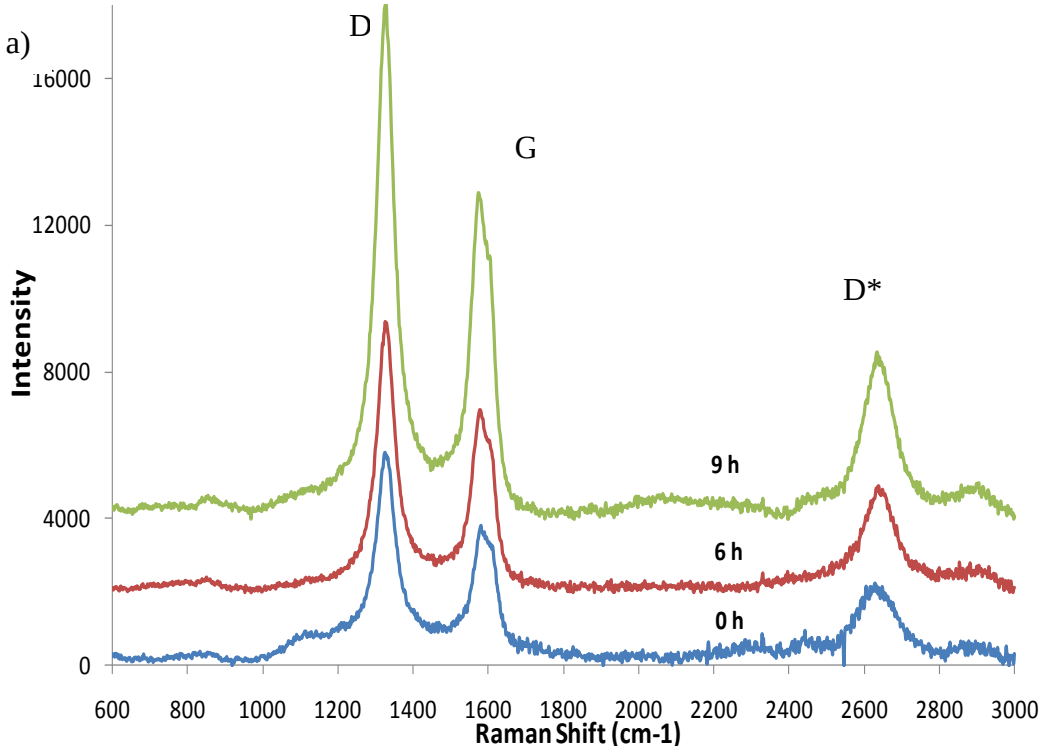

Figure 5.6. Raman spectra analysis for as prepared and treated MWCNTs. a) Raman spectrums for as prepared MWCNT 95% purity and treated for 6 and 9h, b) D and G band ratio versus treatment time.

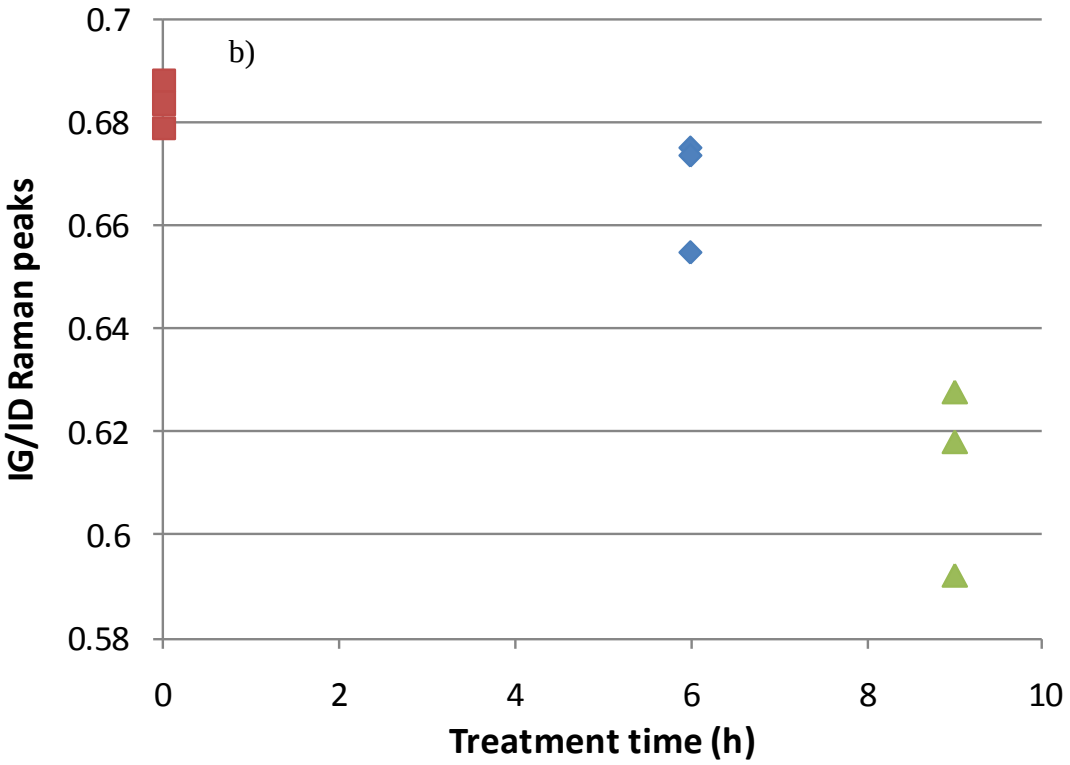

Figure 5.6. Raman spectra analysis for as prepared and treated MWCNTs. a) Raman spectrums for as prepared MWCNT 95% purity and treated for 6 and 9h, b) D and G band ratio versus treatment time (cont).

Table 5-1. Raman lines Intensities obtained for MWCNTs after different time length nitric acid treatment.

Lines	**Position (cm-1)**	**Line intensity 0 hours**			**6hours**			**9 hours**		
IG	1576.7	3534.72	4247.87	954.721	7791.31	4963.64	6230.5	11538.8	8877.21	11571.2
ID	1325.6	5168.62	6254.54	1386.82	11536.5	7366.05	9514.11	19478.5	14139.3	18717.3
IG/ID		0.6839	0.6792	0.6884	0.6754	0.6739	0.6549	0.5924	0.6278	0.6182

5.2. PRODUCTION OF PALLADIUM NANOPARTICLES ON CARBON NANOTUBES BY GAMMA IRRADIATION

During water radiolysis, species such as H•, OH•, H+, H_2O_2, H_2 and electrons in aqueous solution (e_{-aq}) are produced due to high energy radiation. The concentration of species created in this process is given by the G factor which is the number of molecules or radicals produced per 100 eV of radiation energy absorbed. The normally accepted

values of product yields in Co-60 gamma irradiated aqueous solution with neutral pH and ambient temperature are presented in Table 5-2 [47].

Table 5-2. Radical and molecular product yield in gamma irradiated aqueous solutions [47].

Product	G factor (#species/100ev)
H•	0.61
OH•	2.86
H^+	2.70
H_2O_2	0.61
H_2	0.43
e^-_{aq}	2.70

H• and e^-_{aq}, and OH• are very reactive species, the first two are strong reducing agents with redox potentials: V_{NHE} E° (H+/ H•) =-2.3V_{NHE} and E° (H_2O/ e-aq) =-2.87, respectively. Therefore, they can reduce palladium ions present in the solution to a state of zero-valence. The reduction of metal ions in aqueous solutions is a multistep process where atoms in unusual valence states are initially formed. This is followed by further reduction and agglomeration until a stable nanoparticle is obtained. The reduction of Pd (II) in aqueous solution has been previously studied in detail by Michaelis and Henglein, 1992 [48].

On the other hand, $OH^{\bullet}$ radicals are strong oxidizing agents with E° ($OH^{\bullet}$/ H_2O) =+2.8V_{NHE}, thus, bringing metal atoms to a higher oxidation state. Hence, a scavenger of $OH^{\bullet}$ radicals, such as primary or secondary alcohols or formate ions, is added to the solution prior to irradiation. The secondary radicals, products of the reaction between the scavenger and radiolysis species $H^{\bullet}$ and $OH^{\bullet}$, are also strong reducing agents; the reactions are summarized in Table 5-3 [11, 49].

Table 5-3 Reactions of scavenger and radicals and redox potentials of the radical products [11].

Scavenger	Radical	Products	Redox potential
$(CH_3)_2CHOH$	OH•	$(CH_3)_2C•OH + H_2O$	$E°((CH_3)_2CO/(CH_3)2C•OH)$= -1.8VNHE
	H•	$(CH_3)_2C•OH + H_2$	
HCOO-	OH•	$COO- + H_2O$	$E°(CO_2/ COO-)$= -1.9VNHE
	H•	$COO- + H_2$	

The initial solution with water alcohol and $PdCl_2$ showed an orange color at room temperature and became darker after 2 hours approximately. This behavior suggests spontaneous formation of Pd nuclei even before gamma irradiation as proposed by A. Sarkany et al. with G values calculations [50]. However no deposition of palladium nanoparticles was observed before gamma irradiation in his experiments. It was suggested that those seeds provide sites for a combined catalytic/radiolytic reduction of Pd^{2+} during irradiation. In order to verify that no nanoparticles were deposited on the carbon nanotubes before gamma irradiation, the blanks samples were analyzed. The result was that no nanoparticles grew in the CNTs.

The range of doses selected for our experiments between 10kGy and 40 kGy should lead to the generation of $OH^{\bullet}$ and $H^{\bullet}$ radicals in concentration ranges of 2.96×10^{-3}-$1.18x10^{-2}$ mol/dm^3 and 6.21×10^{-4}- $2.53\times10^{-3}mol/dm^3$ respectively. Additionally, according to the stoichiometry in Table 5-3, the amount of isopropanol added to the solution (2:1 water/isopropanol) was enough to scavenge the $OH^{\bullet}$ radicals generated during irradiation. As a result, the net amount of reducing agents produced by gamma irradiation in the dispersion was estimated to be sufficient for a complete reduction of the palladium ions generated from 1mg of $PdCl_2$.

Nanoparticles formed during irradiation tend to coalesce and agglomerate due to the high free surface energy, creating big clusters that eventually precipitate in crystals, thus a stabilizer is needed to maintain a good dispersion of the nanoparticles in the liquid.

Surfactants (i.e., surface-active molecules) such as SDS are a group of molecules exhibiting a strong tendency to adsorb at interfaces. They are described by the presence of both polar (hydrophilic) and nonpolar (hydrophobic) groups. They typically have a

hydrophobic chain, known as a tail, and a hydrophilic group, known as a head. Because CNT are hydrophobic, there is a strong possibility for the hydrophobic interaction between the CNT and the hydrophobic head of the surfactant, consequently resulting in the adherence of the surfactant to the CNT. This interaction leads to a better dispersability of the CNTs in aqueous solutions. The possible interactive mechanism of the surfactant and the CNT is schematically shown in Figure 5.7 [26, 51].

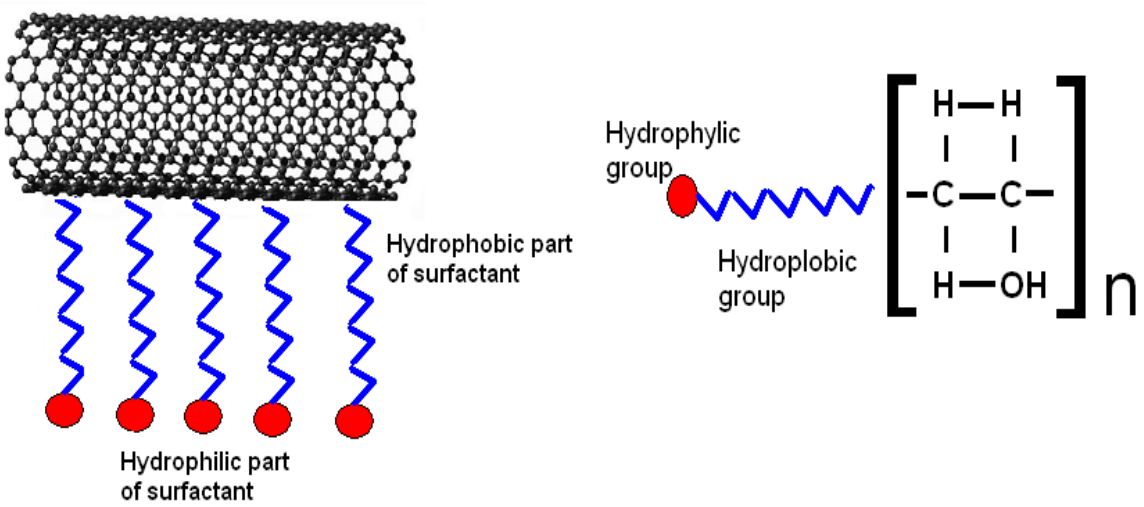

Figure 5.7. Schematic representation of the interaction of carbon nanotubes with a surfactant [26].

The interaction between the surfactant molecule and palladium ions (or any metallic ion) is depicted in Figure 5.8. This configuration is called as reverse micelles; in this case the hydrophilic part of the surfactant is interacting with the ion and the hydrophobic part with the solvent. The concentration of surfactant required to form spherical reverse micelles is determined by the critical micelle concentration, CMC, which is the minimum surfactant concentration necessary to form micelles. The CMC for SDS in pure water is 18mM, this value also varies with the temperature and medium.

.

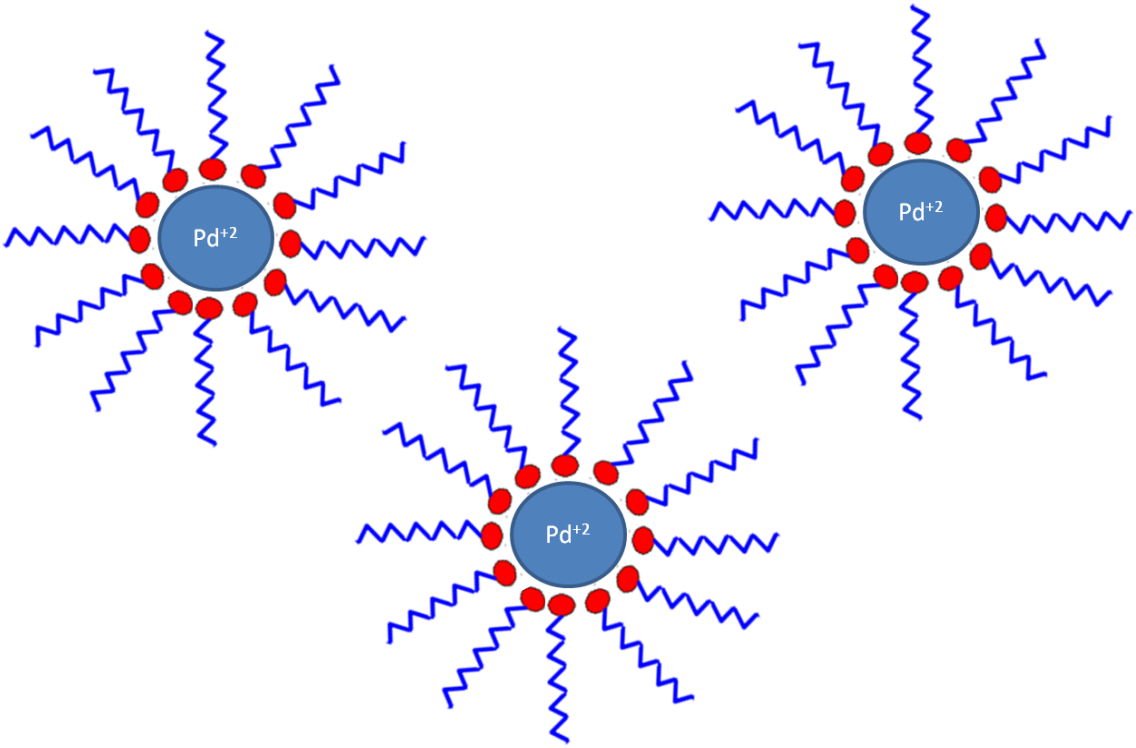

Figure 5.8. Reverse micelles formation of SDS with metallic ions.

Figure 5.9 shows a SEM image of MWCNT after irradiation with water isopropanol ratio of 2:1 prepared as explained in the experimental session with a SDS concentration of 0.015M. In preliminary work, it was found that at very low SDS concentration, less than the CMC of the SDS in water, few or no nanoparticles were obtained; instead large agglomerates were formed due to the lack of dispersion stability [52]. The right amount of SDS allows palladium nanoparticles to form a homogeneous dispersion, leading to the formation of nanoparticles with different sizes at different doses

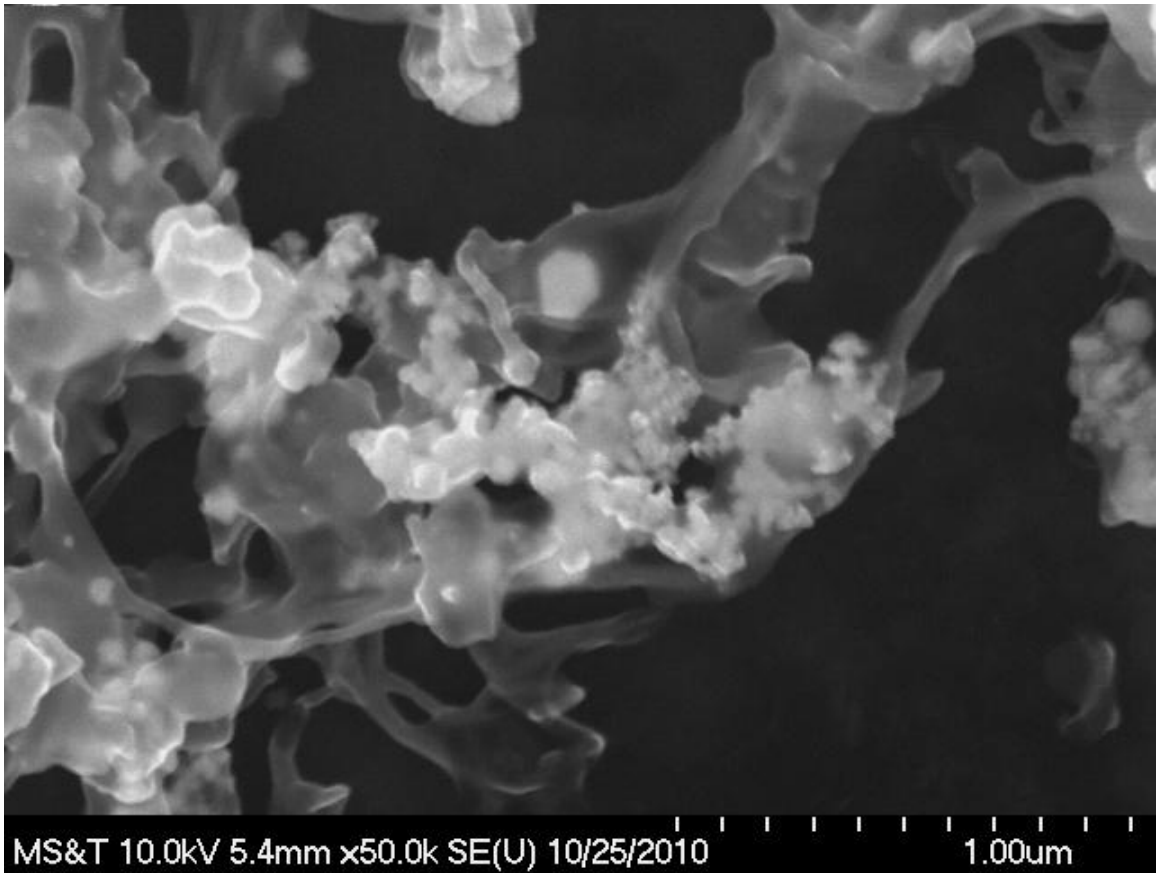

Figure 5.9. SEM image of MWCNTS-Pd after gamma irradiation with 30kGy 15mM SDS

Images were obtained for the different irradiated samples and noticeable variations with dose (10kGy to 40kGy) and amount of SDS (0.05, 0.07, 0.1M) were observed. The proposed mechanism is that an increase in dose leads to a larger amount of reducing agent produced in the solution causing rapid Pd^{+2} reduction forming numerous Pd^{0} seeds. If these early seeds are not stabilized, they would coalesce and no deposition of nanoparticles on the nanotubes is obtained. With the lowest amount of SDS used in these experiments (0.05M) no nanoparticles where obtained except when the highest dose was applied, at 40 kGy sporadic Pd nanoparticles were observed deposited on the nanotubes as shown in Figure 5.10

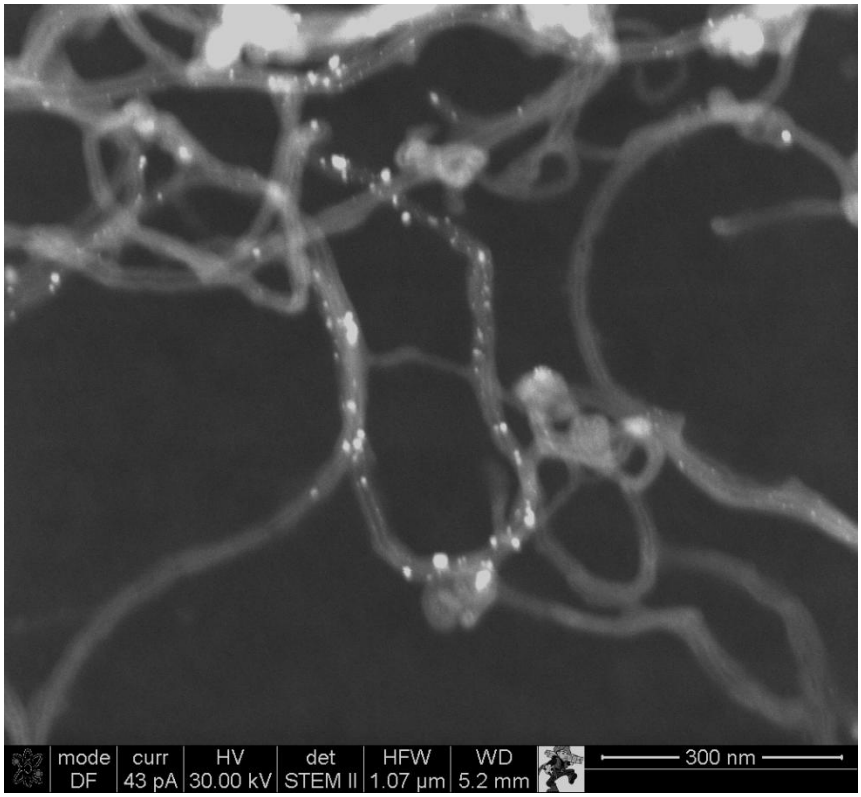

Figure 5.10. STEM image of MWCNTS-Pd after gamma irradiation with 40kGy 0.05M SDS.

By increasing the amount of surfactant, even at low doses, some nanoparticles were observed in the sample. Figure 5.11 shows STEM images of the nanotubes decorated with palladium at 10, 20, 30 and 40 kGy and 0.07M, where the distribution of the nanoparticles with the dose variation is observed.

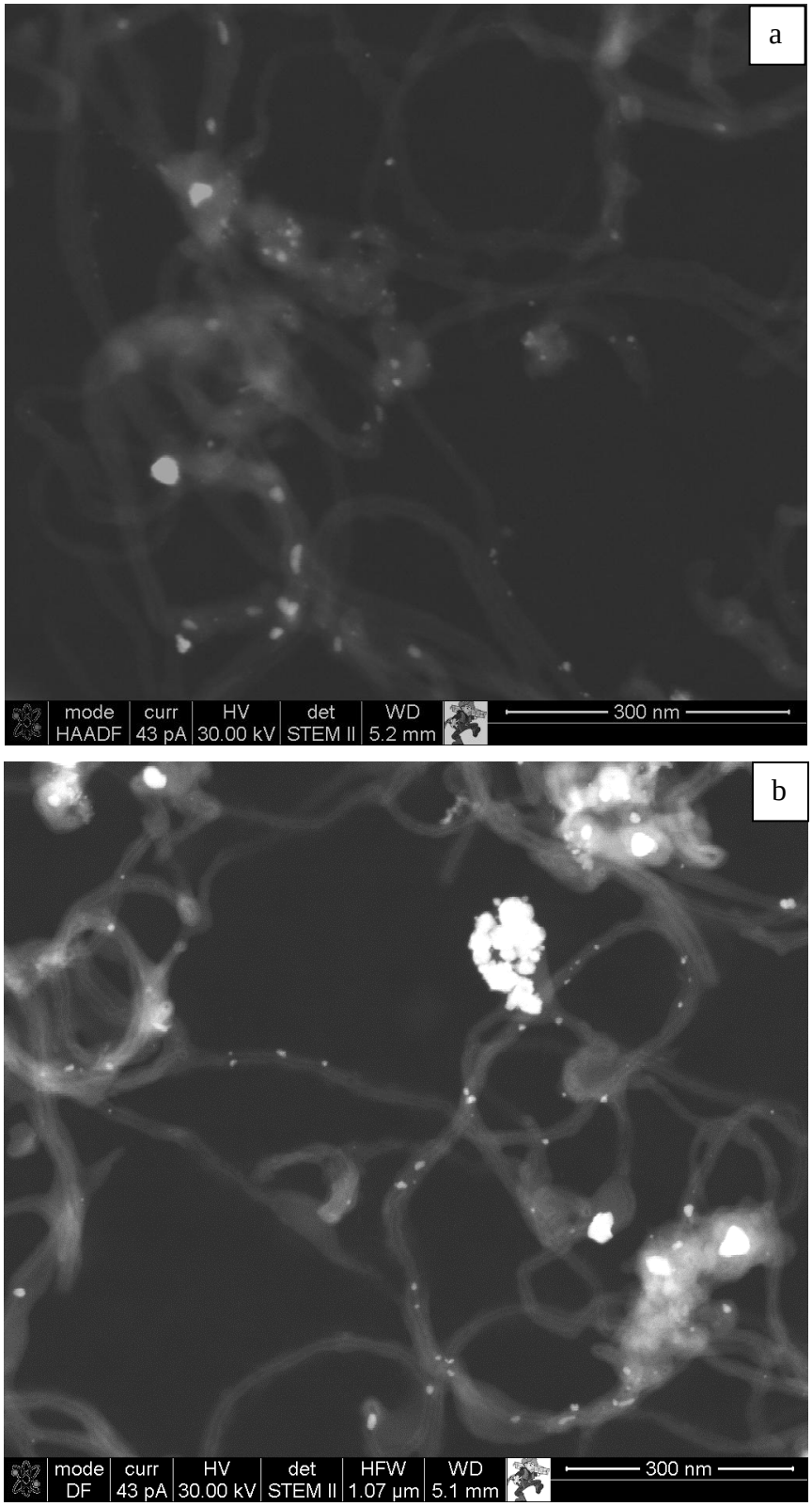

Figure 5.11. STEM images of MWCNT decorated with Pd nanoparticles with 0.07M SDS at different doses. At a)10kGy, b)20kGy, c)30kGy, d) 40kGy .

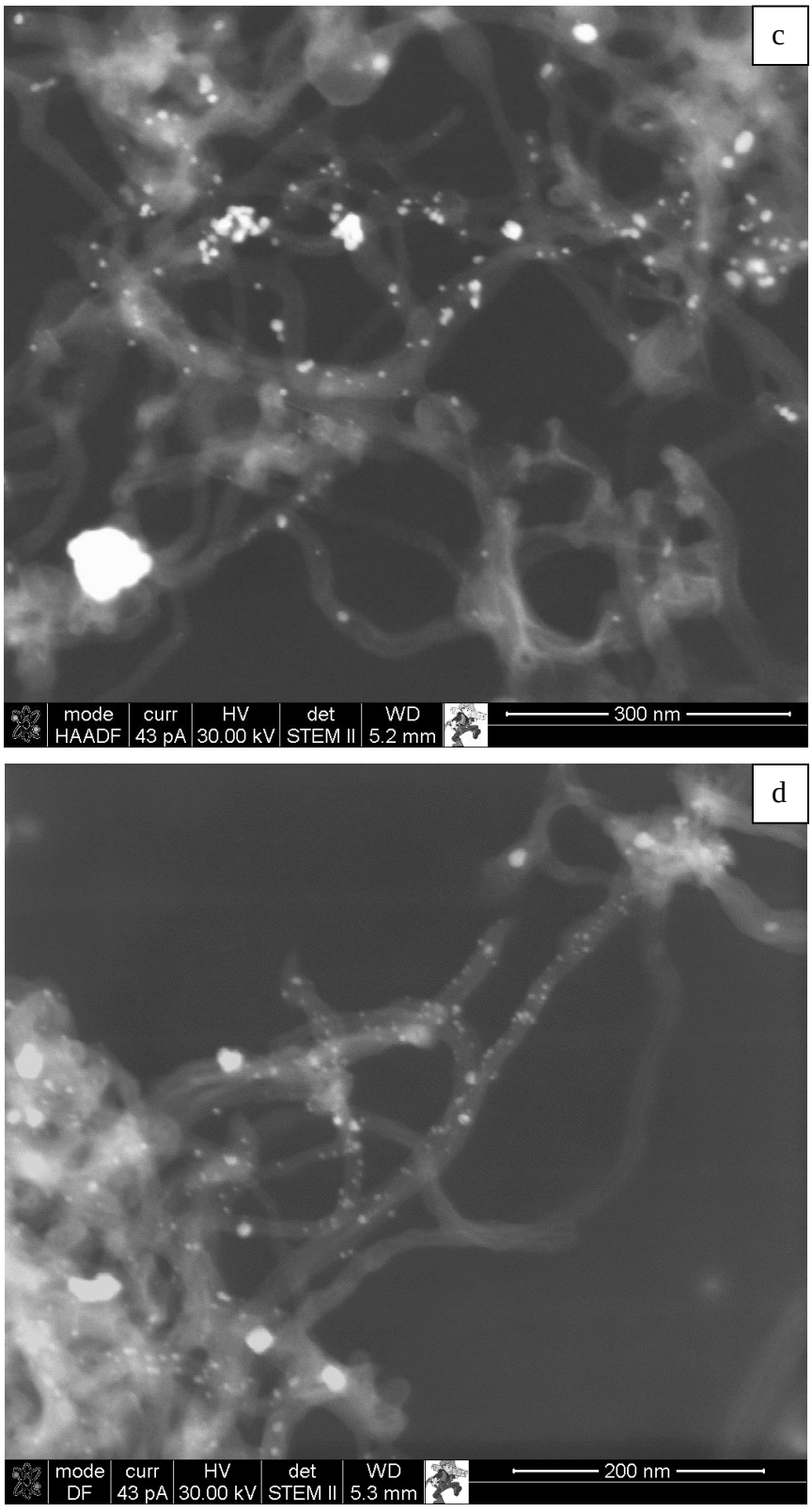

Figure 5.11. STEM images of MWCNT decorated with Pd nanoparticles with 0.07M SDS at different doses. At a) 10kGy, b) 20kGy, c) 30kGy, d) 40kGy (cont).

Besides the nanoparticles obtained on the surface of the carbon nanotubes, bigger particles where also obtained from the process. Histograms of size distribution of palladium nanoparticles at the different doses are shown in Figure 5.12. Two remarkable features are observed with increasing dose are that the frequency of big particles gradually decreases and the peaks position gradually shifts to smaller diameter. The average size (μ) and the standard deviation (σ) of the Pd nanoparticles are shown, where μ1, σ1 and μ2, σ2 correspond to the first and second peak in the histogram respectively.

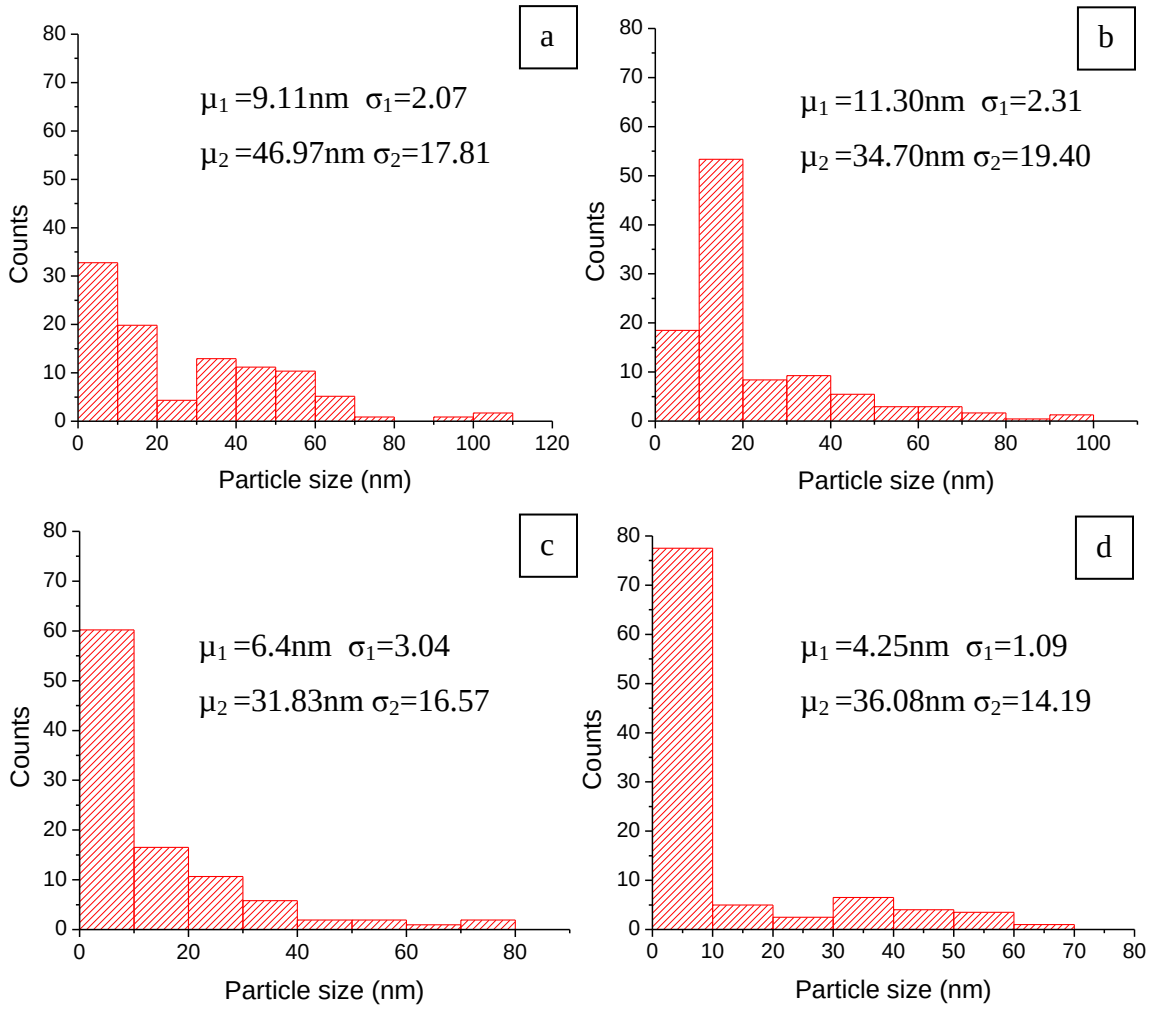

Figure 5.12. Particle size distribution of palladium nanoparticles at a) 10kGy b) 20kGy c) 30kGy, d) 40kGy and e) Plot of particle size vs. dose for μ1.

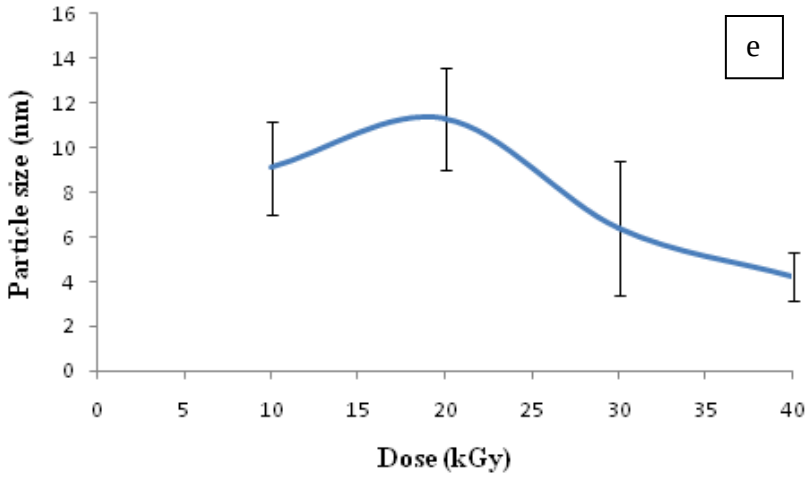

Figure 5.12. Particle size distribution of palladium nanoparticles at a) 10kGy b) 20kGy c) 30kGy, d) 40kGy and e) Plot of particle size vs. dose for µ1 (cont).

The samples containing higher concentration of SDS (0.1M) were also evaluated after irradiation. Nanoparticles were synthesized at 10kGy as observed in Figure 5.13, however at higher doses large agglomerates were observed.

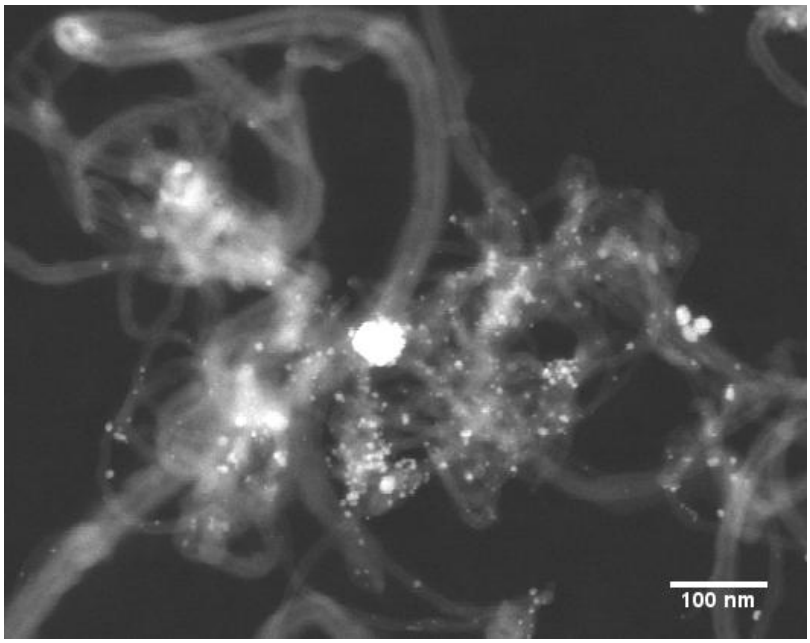

Figure 5.13. STEM images of MWCNT decorated with Pd nanoparticles with 0.1M SDS irradiated at 10kGy.

The sample irradiated at 40 kGy using 0.07M SDS in solution was evaluated with TEM in order to better distinguish the particle size and distribution of the palladium nanoparticles in the nanotubes. Figure 5.14 shows the TEM images obtained in bright field mode.

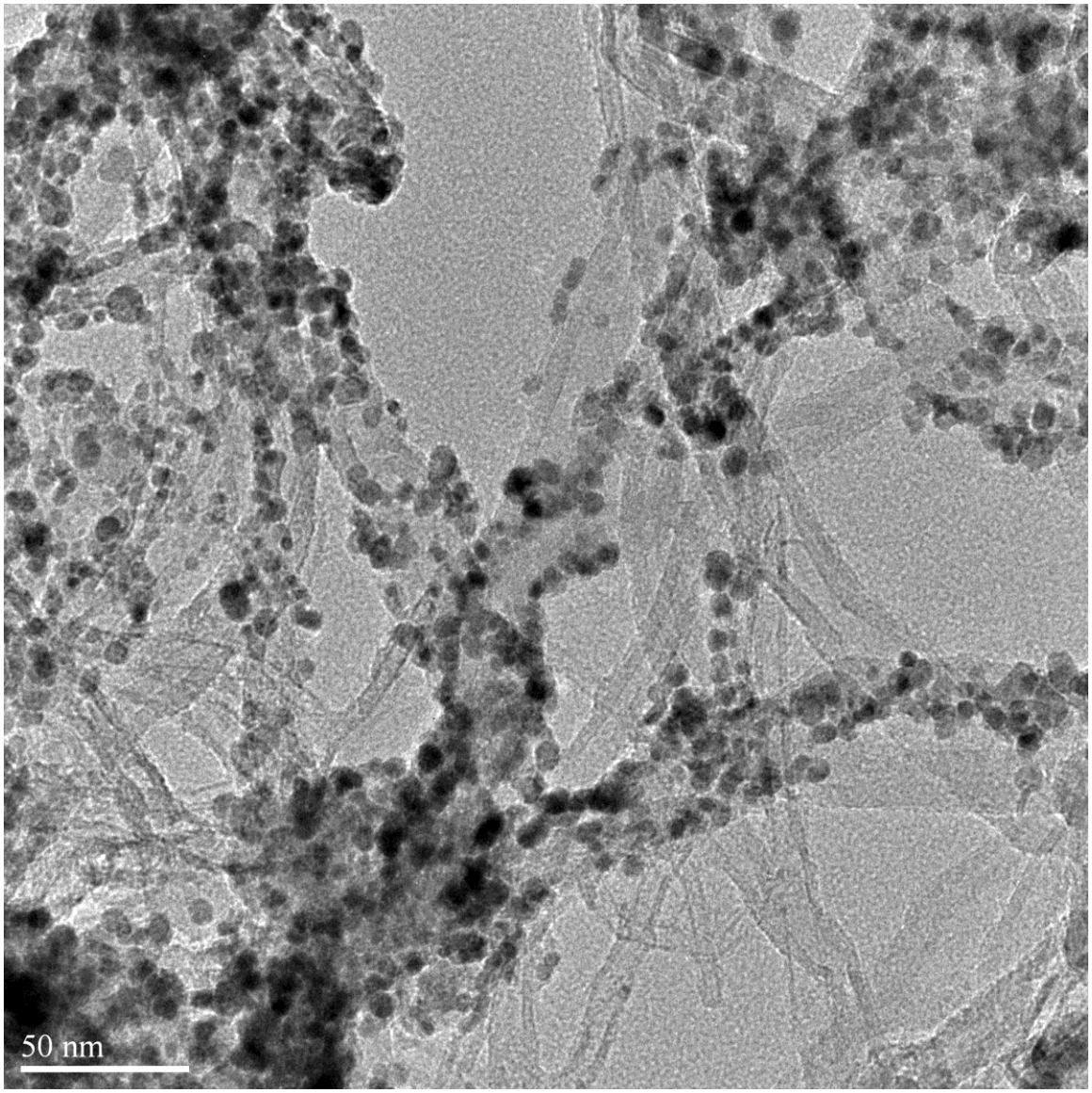

Figure 5.14. TEM images of MWCNT decorated with Pd nanoparticles at 40kGy and 0.07M SDS.

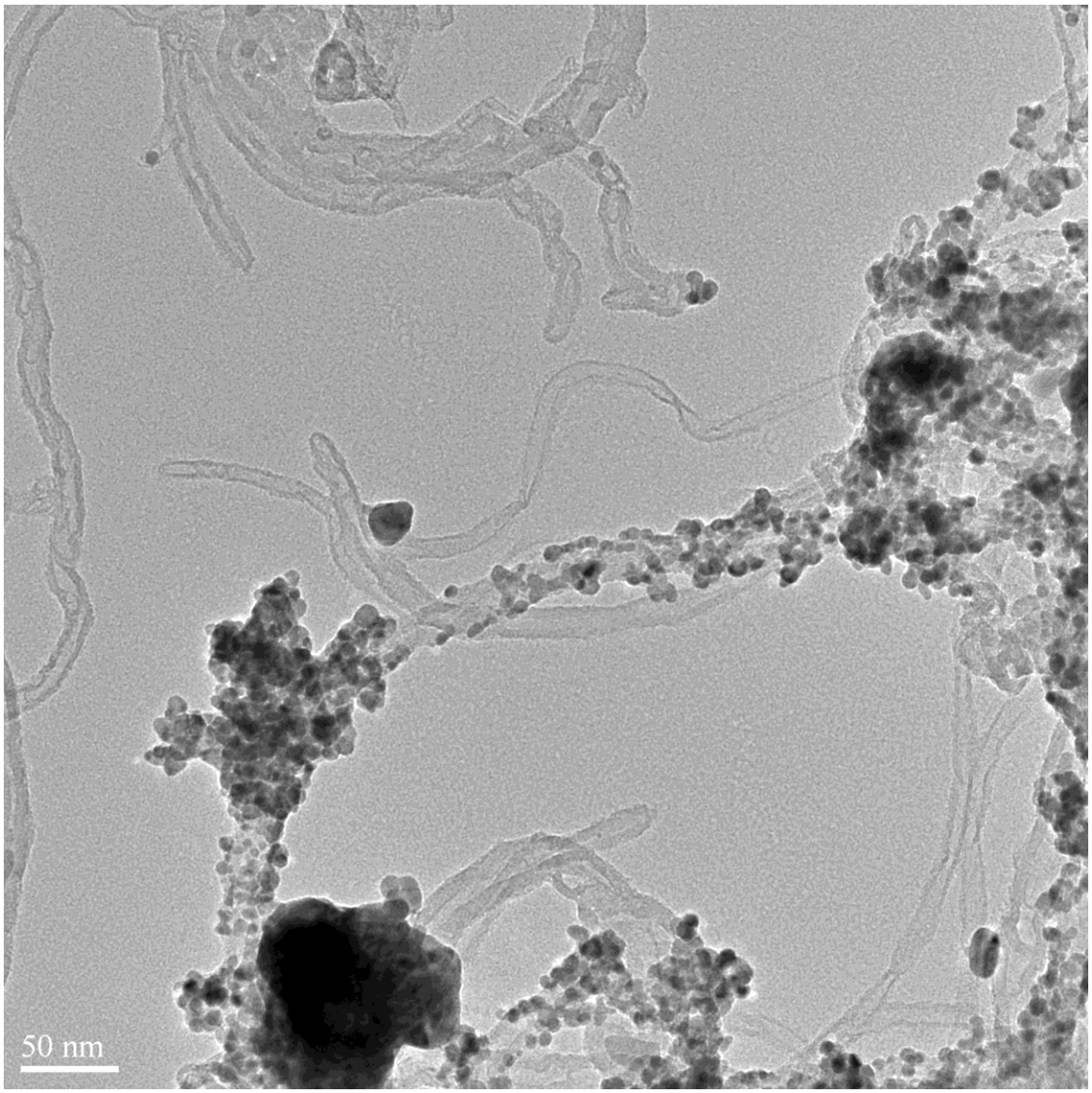

Figure 5.14. TEM images of MWCNT decorated with Pd nanoparticles at 40kGy and 0.07M SDS (cont).

The EDX spectrum shown in Figure 5.15 obtained in STEM mode clearly confirm the presence of palladium at the selected point. Additionally, chemical elements such as carbon (C), oxygen (O) aluminum (Al), copper (Cu) and silicon (Si) were also identified. Cu peaks usually appear in the spectrums when elements with high atomic number as Pd are present in the sample. Once the electrons hit heavy elements, they are scattered through high enough angles and some of them strike the copper grid.

Additionally, silicon peak is due to some x rays that are generated at the semiconductor detector.

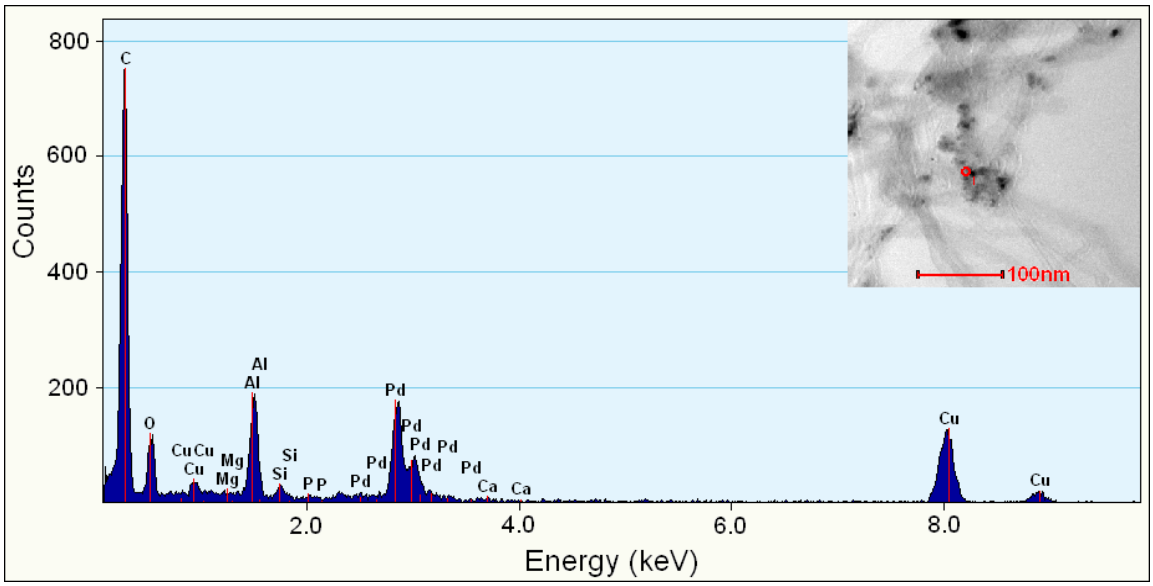

Figure 5.15. EDX points scan of MWCNT adorned with Pd nanoparticles generated by 40kGy gamma radiation dose and 0.07M SDS.

Figure 5.16 shows a high resolution TEM (HRTEM) image that was obtained in bright field mode in order to better visualize the interaction between the nanoparticles and the nanotubes. Palladium has a face centered cubic (FCC) crystalline structure with a d-spacing (d_{111}) of 0.2246nm (ICDD data base, pdf card 00-005-0681). This value was confirmed from the HRTEM image using ImageJ software after a thorough scale calibration as it is shown in Figure 5.17. Additionally, the corresponding FTT spectrum verifies the cubic crystalline structure of the nanoparticle. The measured d_{111} was found to be 0.22nm with a standard deviation of 0.01nm. Therefore, there is an error of 3.7%, which according with previous magnification calibration of the TEM, it falls within the range.

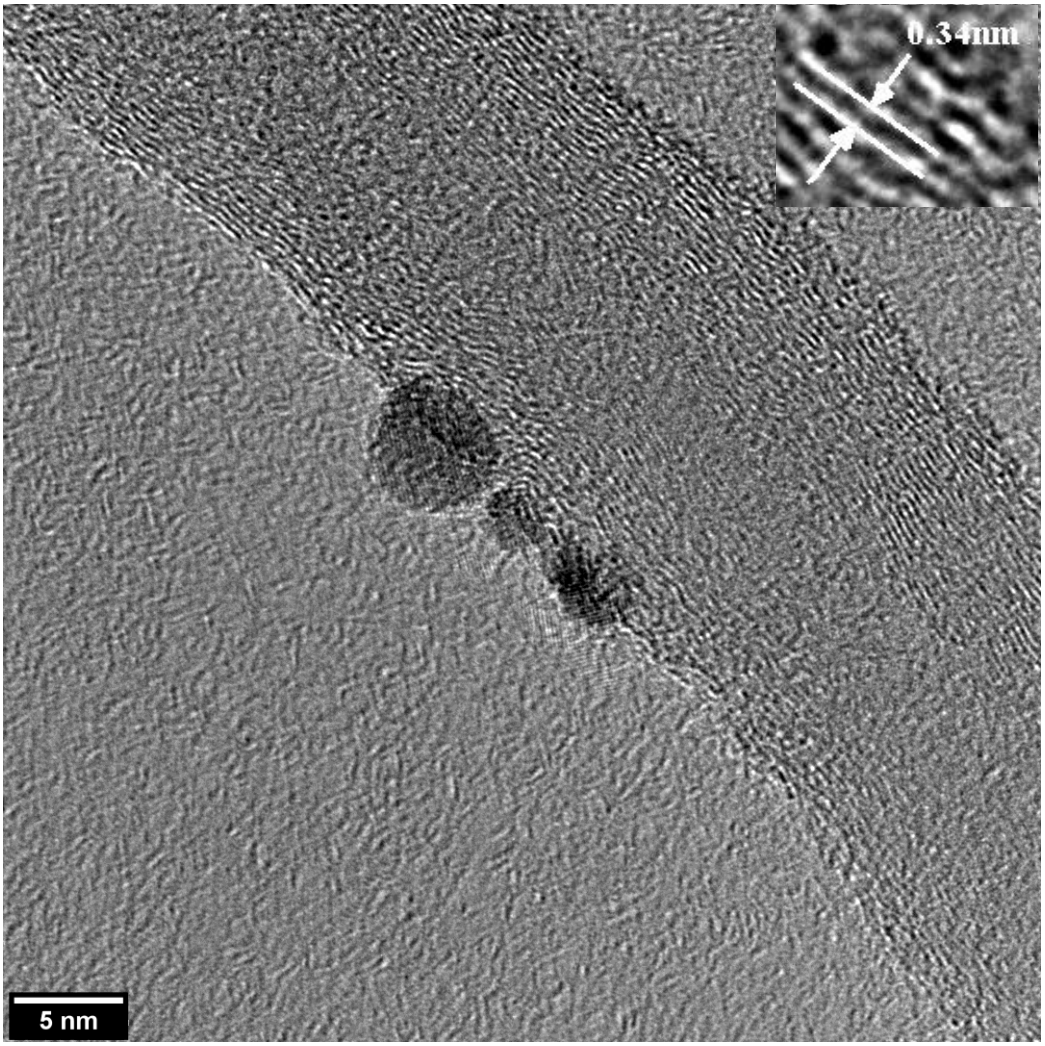

Figure 5.16. High resolution TEM image of MWCNT decorated with Pd nanoparticles.

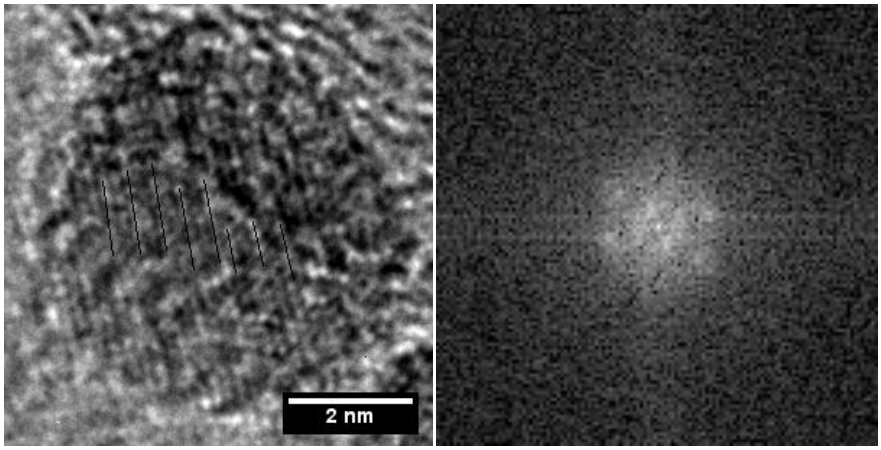

Figure 5.17. High resolution image of Pd nanoparticles and its corresponding FFT.

Figure 5.18 shows XPS spectra obtained after γ-irradiation, where the C-1, O-1s, and Pd-3d doublet are observed. The carbon peak was observed at 284.5eV as seen in Figure 5.18 b). The low intensity peak next to the carbon peak at 285.8 eV indicates a higher binding energy characteristic of COOH groups. This feature confirms the presence of functional groups in the nanotubes. Palladium peaks Pd3d5/2 and Pd3d3/2 become visible at binding energies of 335.9 and 341.1eV respectively which are characteristic of metallic palladium (Pd^0), thus confirming the successful reduction of Pd^{+2} to Pd^0. Pd-C bonds, forming palladium carbide (PdCx), have been reported at binding energies around 282 eV, but no additional features are observed from the spectrum [53]. Thus, no chemical bonds are present between palladium and carbon. On the other hand, low intensity peaks overlapped with the palladium peaks that rise in the side of increasing energy suggests formation of Pd-O bonds, which appear at 336.8eV and 342.2eV. The interaction of Palladium carbon might be explained as PdO- CNTs bonds, supported by the functional groups identified near the carbon peak.

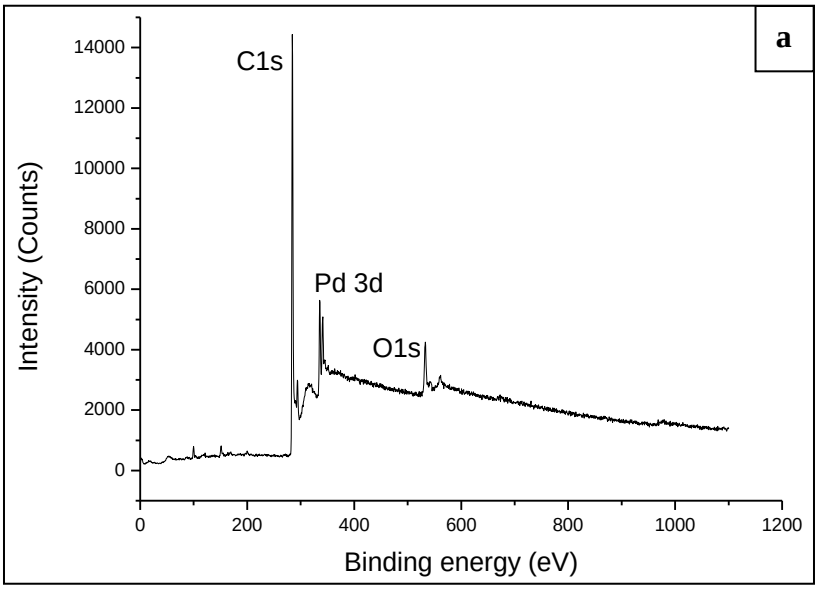

Figure 5.18. XPS spectrum of CNTs-Pd proving the reduction of Pd^{+2} into Pd^0 as well as C and O chemical species. a) general XPS spectra, b) High resolution for C peak and c) High resolution for Pd Peak.

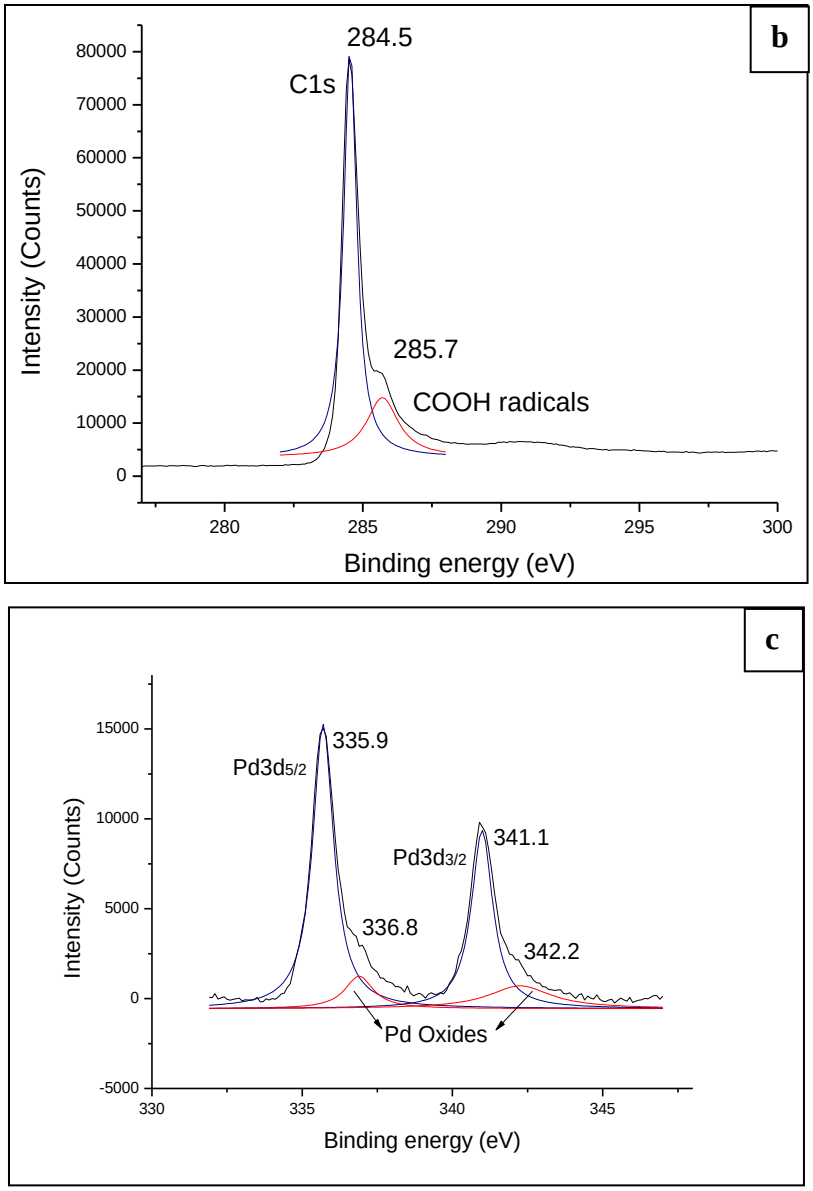

Figure 5.18. XPS spectrum of CNTs-Pd proving the reduction of Pd^{+2} into Pd^{0} as well as C and O chemical species. a) general XPS spectra, b) High resolution for C peak and c) High resolution for Pd Peak (cont).

6. CONCLUSIONS

- Purification of MWCNTs carbon nanotubes with concentrated nitric acid (70%) with refluxing periods of 6 and 9 hours was conducted. The morphology of the treated samples was analyzed with scanning transmission electron microscopy. After 6 hours acid treatment the reduction of the metallic particles and carbonaceous impurities was remarkable. At 9 hours of treatment the oxidation process that takes place in the reaction begins to destroy the nanotubes.
- A complementary analysis of FTIR and Raman Spectroscopy of the as received and acid treated MWCNTs were obtained. This study revealed the formation of carboxyl functional groups (–COOH) and ketone/quinone after the chemical treatment.
- Palladium nanoparticles were successfully synthesized and deposited on the surface of multi-walled carbon nanotubes by gamma irradiation of a solution with a specific water-isopropanol ratio. It is estimated that the irradiation of the precursor solution creates the chemical agents needed for a complete reduction of the Pd ions in the solution. Gamma dose and amount of surfactant were varied during the experiments in order to identify the effect of those variables in the process. Doses from 10 to 40kGy and dispersions with 0.05, 0.07 and 0.1M of SDS were used. The nanostructure was chemical and morphologically evaluated by XPS, STEM and TEM. Using these techniques, metallic Pd was identified and nanoparticles were observed attached to the surface to the MWCNTs. The interaction of Pd-CNT might be explained by the formation of Pd-O on the surface of the nanotubes, but no Pd-C bonds were detected. Samples irradiated at 30 and 40kGy and 0.07M of SDS shows the most uniform distribution of the nanoparticles within the range from 3 to 7nm.

APPENDIX A.

HYDROGEN STORAGE CAPACITY OF MWCNTs TREATED WITH NITRIC ACID

Preliminary analysis of Hydrogen storage of MWCNTs was conducted after chemical treatment with nitric acid as explained in the experimental procedure. Isothermal hydrogen adsorption curves for hydrogen storage capacity of the nanotubes were obtained using a Micromeritics ASAP 2020 (Accelerated Surface Area and Porosimetry analyzer) located at the Chemistry department under Dr. Nicolas Leventis.

The dry samples were subjected to previous degassing process during 12 hours at 100°C. The isothermal adsorption curves were performed at room temperature up to a pressure of 1atm.

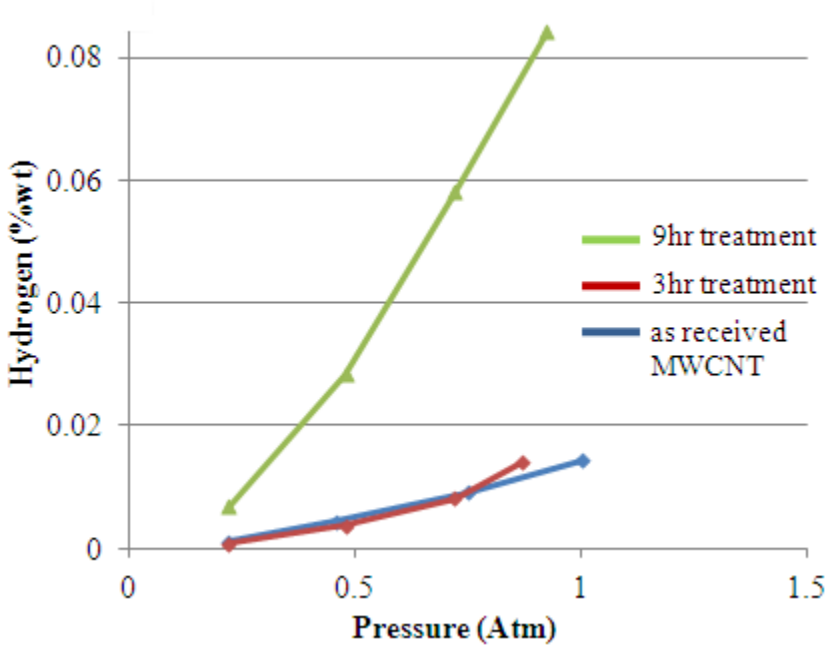

Figure A.1. Hydrogen storage capacity of MWCNTs treated with nitric acid for different periods of time. Measurements obtained up to 1 atm.

Hydrogen storage capacity of the MWCNTs was improved by a factor of 6 with respect to the as received sample. The improvement of the hydrogen storage capacity of the treated nanotubes can be attributed to the opening up of the nanotubes, and the creation of the oxygen functional groups that provide more hydrogen-related sites on the MWNTs.

APENDIX B.

JOURNAL PAPER

Author's Accepted Manuscript

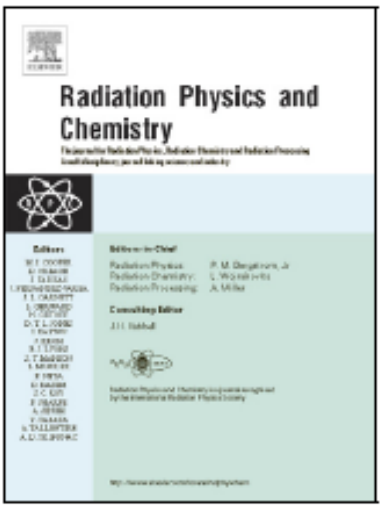

www.elsevier.com/locate/radphyschem

Production of palladium nanoparticles supported on multi-walled carbon nanotubes by gamma irradiation

J.V. Rojas, C.H. Castano

PII: S0969-806X(11)00284-2
DOI: doi:10.1016/j.radphyschem.2011.08.010
Reference: RPC 5356

To appear in: *Radiation Physics and Chemistry*

Received date: 9 June 2011
Accepted date: 19 August 2011

Cite this article as: J.V. Rojas and C.H. Castano, Production of palladium nanoparticles supported on multi-walled carbon nanotubes by gamma irradiation, *Radiation Physics and Chemistry*, doi:10.1016/j.radphyschem.2011.08.010

PRODUCTION OF PALLADIUM NANOPARTICLES SUPPORTED ON MULTI-WALLED CARBON NANOTUBES BY GAMMA IRRADIATION

J. V. Rojas [a], C. H. Castano [a*]

[a] Nuclear Engineering, Missouri University of Science and technology, 301 W. 14th ST, Rolla, MO 65409

jvr45d@mail.mst.edu

[a*] **Corresponding author,** Nuclear Engineering, Missouri University of Science and technology, 222 Fulton Hall, 301 W. 14th ST, Rolla, MO 65409

Phone: +1 (573) 341-6766

Fax: +1 (573) 341-6309

castanoc@mst.edu

Abstract

Palladium nanoparticles were produced and supported on multiwalled carbon nanotubes (MWCNT) by gamma irradiation. A solution with a specific a ratio of 2:1 of water-isopropanol was prepared and mixed with palladium chloride and the surfactant sodium dodecyl sulfate (SDS). The gamma radiolysis of water ultimately produces Pd metallic particles that serve as nucleation seeds. Isopropanol is used as an ion scavenger to balance the reaction, and the coalescence of the metal nanoparticles was controlled by the addition of SDS as a stabilizer. The size and distribution of nanoparticles on the carbon nanotubes (CNT) were studied at different surfactant concentration and radiation doses. SEM, STEM and XPS were used for morphological, chemical, and structural characterization of the nanostructure. Nanoparticles obtained for doses between 10-40kGy, ranged in size between 5 to 30nm. The smaller nanoparticles were obtained at the higher doses and vice versa. Histograms of particle size distributions at different doses are presented.

Keywords: carbon nanotubes, nanoparticles, palladium, gamma irradiation, radiation induced chemistry

1. Introduction

Since their discovery in 1991, carbon nanotubes have been widely investigated due to their outstanding chemical, optical, electrical and mechanical properties that make them suitable for a variety of applications. Carbon nanotube composites, electronic devices, field emitters, and sensors are some of the uses currently being investigated (Baughman et al., 2002). In addition, it has been proposed that single and multiwalled carbon nanotubes (SWCNTs and MWCNTs) are expected to achieve high hydrogen storage due to their high surface area and pore volume (Jain, 2009). Due to various factors affecting hydrogen storage capacity including geometry, purity, and manufacturing process, a wide variation in hydrogen capacity of carbon nanotubes has been reported with low repeatability and reproducibility of the results (Darkrima et al., 2002; Yurum et al., 2009).

Several approaches have been suggested to improve the hydrogen storage capacity of carbon nanotubes. Lipson et al. in 2008 synthesized a new nanocomposite material with SWCNT encapsulated by thin electroplated Pd layers on top of a massive Pd foil, enhancing the hydrogen uptake of the system. According to that paper, the SWCNT system studied had a capacity of 8-12 % wt H_2 (Lipson et al., 2008). Unfortunately, the presence of the massive Pd substrate supporting the nanophase eliminated the mass advantage achieved by the enhanced CNT hydrogen capacity. Hence, incorporation of metallic nanoparticles on the surface of CNTs is currently being investigated at the Missouri University of Science and Technology as a means to achieve a similar structure without the presence of the massive Pd substrate. Promising results have been previously reported in this area (Suttisawat et al., 2009).

Numerous methodologies have been developed for the decoration of CNTs with Pd nanoparticles, including electroless deposition, thermal decomposition, and vapor deposition (Georgakilas et al., 2007; Karousis et al., 2008; Bera et al., 2004). Some of the methods for adding metallic nanoparticles to the nanotubes use an aqueous medium which contains a metal precursor salt and a reducing agent mixed together (Lee et al., 2007). Besides those chemical methods, radiation chemistry has also contributed to the advances in this area since the reduction of metal precursors may also be achieved by radiolytic synthesis in various solutions. This process has the advantage of simple physicochemical conditions that lead to homogeneous

reduction and nucleation of the metallic nanoparticles (Belloni et al., 1998; Remita and Remita, 2010). Work has been previously conducted specifically with Pd to study the formation of the colloidal Pd particles by gamma irradiation (Michaelis and Henglein, 1992). In such work, it was found that a polymer was often required to serve as support of the nascent Pd particles.

In this work, a method to produce Pd nanoparticles supported on multiwalled CNTs using gamma irradiation is presented. The resulting nanostructure was characterized with STEM, TEM, and XPS, which yielded information about the morphology of the nanoparticles and their interaction with the nanotubes.

2. Experimental Procedure

In order to produce palladium nanoparticles supported on MWCNT, palladium chloride ($PdCl_2$) was used as a metal precursor. MWCNT with 3-20 nm outside diameter, 1-3 nm inside diameter, 0.1-10 micron long and 95.5% of purity, Palladium chloride ($PdCl_2$) and sodium dodecyl sulfate (SDS, $C_{12}H_{25}SO_4Na$) were purchased from Alfa Aesar. An aqueous solution with palladium chloride, MWCNT, SDS, water, and isopropanol was prepared. For this solution, 12 mg of $PdCl_2$ and 12mg of carbon nanotubes were added to 12ml of distillated water-isopropanol (2:1 v/v) and sonicated for 30 minutes. This results in a concentration of isopropanol and palladium ions into solution of 4.4 and $5.6x10^{-3}$ mol/dm^3 respectively. The dispersion was distributed in sample vials containing various amounts of SDS resulting in concentrations of 14.6mg/ml (0.05 mol/dm^3), 20.6 mg/ml (0.07 mol/dm^3) and 29.7mg/ml (0.1 mol/dm^3). The samples were placed in an ultrasonic bath for 30 minutes in order to achieve further dispersion and finally degassed with argon to remove oxygen. The samples were irradiated by Cobalt-60 gamma rays with doses of 10, 20, 30 and 40 kGy at a dose rate of 10kGy/hr (1Mrad/hr). After irradiation, the dispersions were washed with deionized water several times to remove the excess of surfactant and finally stored in acetone. Identical samples were also prepared but not irradiated, to test that no spontaneous formation of Pd nanoparticles in the CNTs was taking place.

In order to analyze the morphology of the resulting nanostructures, a Helios NanoLab 600 in STEM mode at 30kV and a TEM TECNAI F20 at 200kV were used. The samples were prepared

by diluting a small amount of the irradiated dispersion in acetone and sonicating for 30 minutes. Several drops of the solution were subsequently deposited on a carbon coated copper grid. The oxidation state of palladium in the samples was identified by XPS. Spectra were obtained with a Kratos Axis 165 Photoelectron Spectrometer, where a silicon wafer was used as a substrate in which to deposit the sample.

3. Results and Discussion

During water radiolysis, species such as H•, OH•, H^+, H_2O_2, H_2 and electrons in aqueous solution (e^-_{aq}) are produced due to high energy radiation. The concentration of species created in this process is given by the G factor which is the number of molecules or radicals produced per 100 eV of radiation energy absorbed. Product yields in gamma irradiated aqueous solution are G(•H)=0.61, G(OH•)=2.86, G(H^+)=2.70, G(H_2O_2)=0.61, G(H_2)=0.43, G(e^-_{aq})=2.7 (Appleby and Schwarz, 1969).

e^-_{aq}, H•, and OH• are very reactive species, the first two are strong reducing agents with redox potentials: E° (H_2O/ e^-_{aq}) =-2.87V_{NHE} and E° (H^+/ H•) =-2.3V_{NHE}, respectively. Therefore, they can reduce palladium ions present in the solution to a state of zero-valence. The reduction of metal ions in aqueous solutions is a multistep process where atoms in unusual valence states are initially formed. This is followed by further reduction and agglomeration until a stable nanoparticle is obtained. The reduction of Pd (II) in aqueous solution has been previously studied in detail by Michaelis and Henglein, 1992.

On the other hand, OH• radicals are strong oxidizing agents with E° (OH•/ H_2O) =+2.8V_{NHE}, thus, bringing metal atoms to a higher oxidation state. Hence, a scavenger of OH• radicals, such as primary or secondary alcohols or formate ions, is added to the solution prior to irradiation. Equations (1) and (2) show the reaction between the scavenger and radiolysis species H• and OH•. The secondary radicals, products of these reactions, are also strong reducing agents as can be seen from their reduction potential. (Belloni et al., 1998; Remita and Remita, 2010).

$(CH_3)_2CHOH + OH^\bullet\ (H^\bullet) \rightarrow (CH_3)_2C^\bullet OH + H_2O\ (H_2)$ (1)

E°($(CH_3)_2CO$/$(CH_3)_2C^\bullet OH$)= -1.8VNHE

$HCOO^- + OH^\bullet (H^\bullet) \rightarrow COO^{\bullet-} + H_2O (H_2)$ (2)

$E°(CO_2/ COO-) = -1.9VNHE$

The initial solution with water, alcohol, and $PdCl_2$ showed an orange color at room temperature and became darker after approximately 2 hours. This behavior suggests spontaneous formation of Pd nuclei even before gamma irradiation (Sarkany et al., 2005). We conducted a blank experiment to verify that the nucleation of Pd on CNTs was due to γ-irradiation and not spontaneous reduction. The blank samples were then analyzed in STEM, and there were no nanoparticles observed in the non-irradiated CNTs. Apparently, the spontaneous formation of free Pd particles is not related to the nanoparticles formed on the nanotubes under gamma irradiation.

The range of doses selected for our experiments between 10kGy and 40 kGy should lead to the generation of $OH^\bullet$ and $H^\bullet$ radicals in concentration ranges of 2.96×10^{-3}-1.18×10^{-2} mol/dm^3 and 6.21×10^{-4}- 2.53×10^{-3}mol/dm^3 respectively. Additionally, according to the stoichiometry from equations (1) and (2), the amount of isopropanol added to the solution (2:1 water/isopropanol) was enough to scavenge the $OH^\bullet$ radicals generated during irradiation. As a result, the net amount of reducing agents produced by gamma irradiation in the dispersion was estimated to be sufficient for a complete reduction of the palladium ions generated from 1mg of $PdCl_2$.

Figure 1 shows the STEM image of the MWCNTs before irradiation, where their clean surface is clearly observed. After irradiation, preliminary results showed that at very low SDS concentration (less than 18mM of SDS) few or no nanoparticles were obtained; instead, large agglomerates were formed due to the lack of dispersion stability (Rojas and Castano, 2011). Nanoparticles formed during irradiation tend to coalesce and agglomerate due to the high free surface energy, creating big clusters that eventually precipitate in crystals. Thus, a stabilizer is needed to maintain a good dispersion of the nanoparticles in the liquid. Since SDS is an anionic surfactant, it helps to obtain a homogeneous dispersion and stabilize the nanoparticles created during the reaction. The right amount of SDS allows palladium nanoparticles to form a

homogeneous dispersion, allowing the formation of nanoparticles with different sizes at different doses.

Images were obtained for the different irradiated samples and noticeable variations with dose (10kGy to 40kGy) and amount of SDS (0.05, 0.07, 0.1M) observed. The proposed mechanism is that an increase in dose leads to a larger amount of reducing agent produced in the solution, causing rapid Pd^{+2} reduction and forming numerous Pd^{0} seeds. If these early seeds are not stabilized, they would coalesce and no deposition of nanoparticles on the nanotubes occurs. With the lowest amount of SDS used in these experiments (0.05M) no nanoparticles were obtained except when the highest dose was applied. At 40 kGy, sporadic Pd nanoparticles were observed to be deposited on the nanotubes. By increasing the amount of surfactant, even at low doses, some nanoparticles were observed in the sample. Figure 2 shows STEM images of the nanotubes decorated with palladium at 10, 20, 30 and 40 kGy respectively and 0.07M of SDS; a distribution of nanoparticles with variation of the dose is observed. An analysis of these nanoparticles' distribution is presented in Figure 3.

Notice that besides nanoparticles obtained on the surface of the carbon nanotubes, a few bigger particles where also obtained at all irradiation doses. These bigger particles cause, in the histograms of Figure 3, a bimodal distribution of palladium nanoparticles sizes, which is more clearly seen in Figures 3A and 3D. The average size (μ) and the standard deviation (σ) of the Pd nanoparticles are shown in Figure 3 as well. μ_1, σ_1 and μ_2, σ_2 correspond to the statistical analysis of the small and big nanoparticles respectively. Two remarkable features observed with the dose increasing are that the frequency of big particles gradually decreases and the peaks position gradually shifts to smaller diameters.

The sample irradiated at 40 kGy using 0.07M SDS in solution was evaluated with TEM in order to better distinguish the particle size and distribution of the palladium nanoparticles in the nanotubes. Figure 4 shows the TEM images obtained in bright field mode.

The EDX spectrum shown in Figure 5 obtained in STEM mode clearly confirms the presence of palladium at the selected point. Additionally, chemical elements such as carbon (C), oxygen (O)

aluminum (Al), copper (Cu) and silicon (Si) were also identified. Cu peaks usually appear in the spectrums when elements with high atomic number, such as Pd, are present in the sample. Once the electrons hit heavy elements, they are scattered through high enough angles and some of them strike the copper grid. Additionally, the silicon peak is due to some X-rays that are generated at the semiconductor detector.

Figure 6 shows XPS spectrums obtained after γ-irradiation, where the C-1, O-1s, and Pd-3d doublets are observed. The carbon peak was observed at 284.5eV as seen in Figure 6B. The low intensity peak next to the carbon peak at 285.8 eV indicates a higher bonding energy, which is characteristic of COOH groups. This feature confirms the presence of functional groups in the nanotubes. Palladium peaks Pd3d5/2 and Pd3d3/2 become visible at binding energies of 335.9 and 341.1eV respectively. These are characteristic of metallic palladium (Pd^0) as shown in Figure 6C, thus confirming the successful reduction of Pd^{+2} to Pd^0. Pd-C bonds, forming palladium carbide (PdCx) have been reported at binding energies around 282 eV, but no additional features are observed from the spectrum. Thus, no chemical bonds are present between palladium and carbon. On the other hand, low intensity peaks overlapping with the palladium peaks that rise in the side of increasing energy suggests formation of Pd-O bonds, which appear at 336.8eV and 342.2eV. The interaction of Palladium and carbon might be explained as PdO- CNTs bonds, supported by the functional groups identified near the carbon peak.

4. Conclusions

Palladium nanoparticles were successfully synthesized and deposited on the surface of multiwalled carbon nanotubes by gamma irradiation of a solution with a specific water-isopropanol ratio. It is estimated that the irradiation of the precursor solution creates the chemical agents needed for a complete reduction of the Pd ions in the solution. Gamma dose and amount of surfactant were varied during the experiments in order to identify the effect of those variables in the process. Doses from 10 to 40kGy and dispersions with 0.05, 0.07 and 0.1M of SDS were used. The nanostructure was chemical and morphologically evaluated by XPS, STEM and TEM. Using these techniques, metallic Pd was identified and nanoparticles were observed attached to the surface to the MWCNTs. The interaction of Pd-CNT might be explained by the formation of

Pd-O on the surface of the nanotubes, but no Pd-C bonds were detected. Samples irradiated at 30 and 40kGy and 0.07M of SDS show the most uniform distribution of the nanoparticles within the range from 3 to 7nm.

Acknowledgements

This work is being financed by the University of Missouri Research Board with the support of the Missouri S&T Nuclear Engineering Department and the Energy Research and Development Center (ERDC). Additional assistance has been received from the Materials Research Center (MRC) in the materials characterization. We also would like to acknowledge Dr. Stoyan Toshkov at the Nuclear Radiation Lab, University of Illinois Urbana Champaign, for his support doing the sample irradiations.

References

Appleby, A., Schwarz, H. A., 1969. Radical and molecular yields in water irradiated by gamma rays and heavy ions. J. Phys. Chem. 73 (6), 1937–1941.

Baughman, R. H., A. A. Zakhidov, W. A. de Heer, 2002. Carbon Nanotubes—the Route toward Applications. Science. 297, 787-792.

Belloni J., Mostafavi, M., Remita, H., Marignier, J.-L., and Delcourt, M.-O., 1998. Radiation-induced synthesis of mono- and multi-metallic clusters and Nanocolloids. New J. Chem. 1239-1255.

Bera, D., Kuiry, S. C., McCutchen, M., and Seal, S., 2004. In situ synthesis of carbon nanotubes decorated with palladium nanoparticles using arc-discharge in solution method. J. Appl. Phys. 96 (9), 5152-5157.

Darkrima, F. L., Malbrunota, P., Tartagliab, G.P., 2002. Review of hydrogen storage by adsorption in carbon nanotubes. Int. J. Hydrogen Energy. 27, 193–202.

Georgakilas, V., Gournis, D., Tzitzios, V., Pasquato, L., Guldi, D. M. and Prato, M., 2007. Decorating carbon nanotubes with metal or semiconductor nanoparticles. J. Mater. Chem. 17, 2679–2694.

Jain, I.P., 2009. Hydrogen the fuel for 21st century. Int. J. Hydrogen Energy. 34, 7368–7378.

Karousis, N., Tsotsou, G.-E., Evangelista, F., Rudolf, P., Ragoussis, N., and Tagmatarchis N., 2008. Carbon Nanotubes Decorated with Palladium Nanoparticles: Synthesis, Characterization, and Catalytic Activity. J. Phys. Chem. C. 112, 13463–13469.

Lee, C.-L., Huang, Y.-C., Kuo, L.-C., Lin, Y.-W., 2007. Preparation of carbon nanotube-supported palladium nanoparticles by self-regulated reduction of surfactant. Carbon. 45, 203–228.

Lipson, A. G., Lyakhov, B. F., Saunin, E. I., and Tsivadze, A. Yu., 2008. Evidence for large hydrogen storage capacity in single-walled carbon nanotubes encapsulated by electroplating Pd onto a Pd substrate. Phys. Rev. B: Condens. Matter. 77, 081405 1-4.

Michaelis, M., Henglein, A., 1992. Reduction of Pd(II) in Aqueous Solution: Stabilization and Reactions of an Intermediate Cluster and Pd Colloid Formation. J. Phys. Chem. 96, 4719-4724.

Remita, H., Remita, S., 2010. Metal cluster and Nanomaterials: Contribution of radiation chemistry, in: Wishart, J.F., Rao, B.S.M (Eds.), Recent trends in radiation chemistry. World Scientific Publishing Co., Singapore, pp. 347-383.

Rojas, J., Castano, C. H., 2011. Production and Characterization of Supported Transition Metal Nanoparticles on Multi-Walled Carbon Nanotubes Functionalized by Gamma Irradiation and Chemical Processes. Supplemental Proceedings: Materials Processing and Energy Materials TMS. 1, 237-244.

Sarkany, A., Papp, Z., Sajo, I., Schay, Z., 2005. Unsupported Pd nanoparticles prepared by gamma-radiolysis of $PdCl_2$. Solid State Ionics. 176, 209–215.

Suttisawat, Y., Rangsunvigit, P., Kitiyanan, B., Williams, M., Ndungu, P., Lototskyy, M.V., Nechaev, A., Linkov, V., Kulprathipanja, S., 2009. Investigation of hydrogen storage capacity of multi-walled carbon nanotubes deposited with Pd or V. Int. J. Hydrogen energy. 34, 666 –6675.

Yurum, Y., Taralp, A., Veziroglu, T. N., 2009. Storage of hydrogen in nanostructured carbon materials. Int. J. Hydrogen Energy. 34, 3784–3798.

Figure Captions:

Figure 1. STEM of Multiwalled Carbon nanotubes as received, at a magnification of 65kX

Figure 2. STEM images of MWCNT decorated with Pd nanoparticles with 0.07M SDS a) 10kGy b) 20kGy c) 30kGy and d) 40kGy

Figure 3. Particle size (diameter-nm) distribution of palladium nanoparticles at a) 10kGy b) 20kGy c) 30kGy and d) 40kGy with 0.07M of SDS

Figure 4. TEM images of MWCNT decorated with Pd nanoparticles at 40kGy and 0.07M SDS

Figure 5. EDX point scan of MWCNT adorned with Pd nanoparticles 40kGy and 0.07M SDS

Figure 6. a) XPS spectrum of CNTs-Pd proving the reduction of Pd^{+2} into Pd^{0}; b) High resolution of C peak; c) high resolution of Pd peak.

Figure 1.

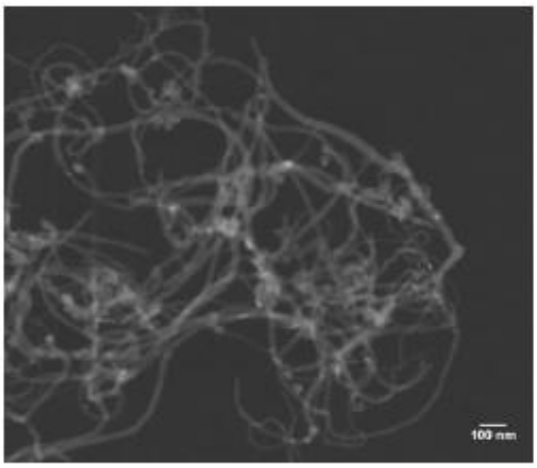

Figure 2.

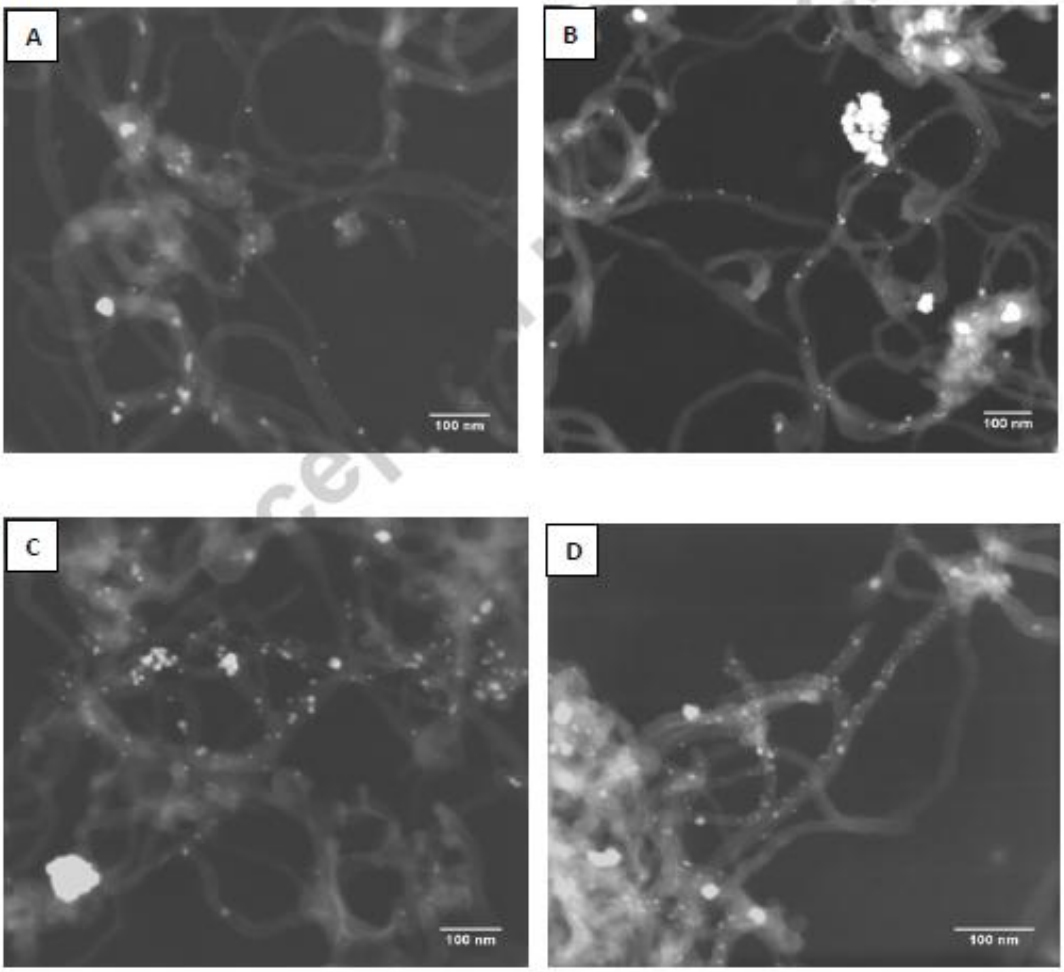

Figure 3.

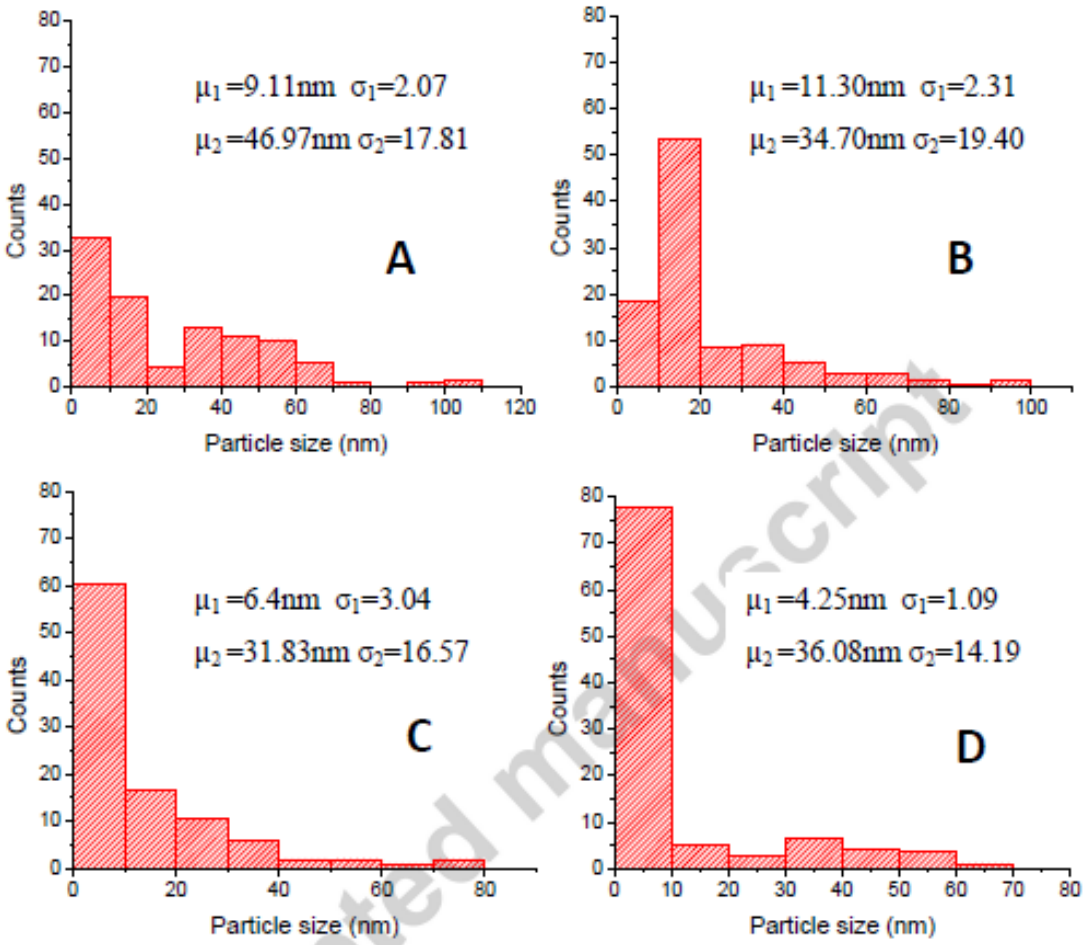

Figure 4.

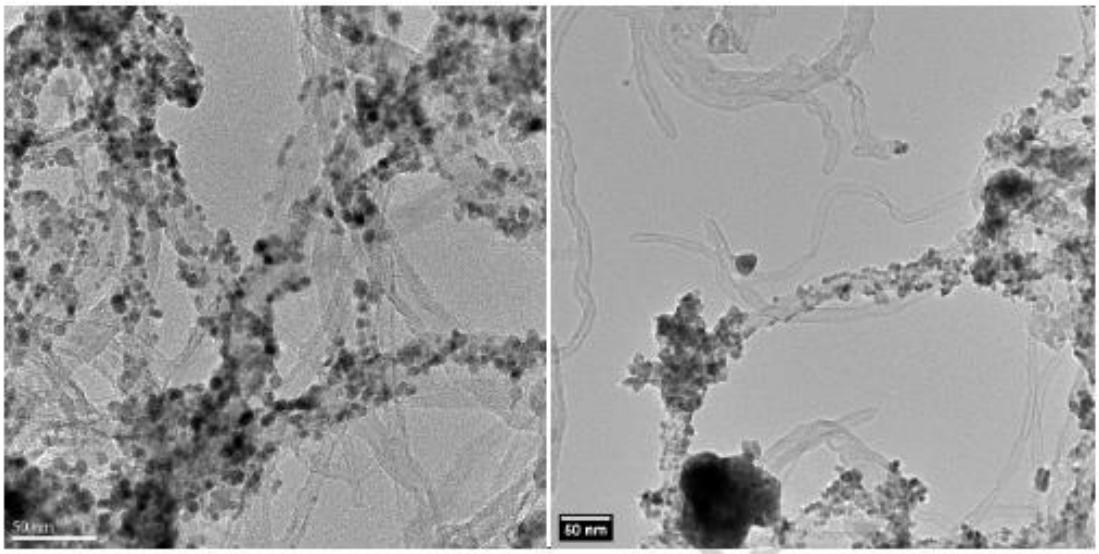

Figure 5.

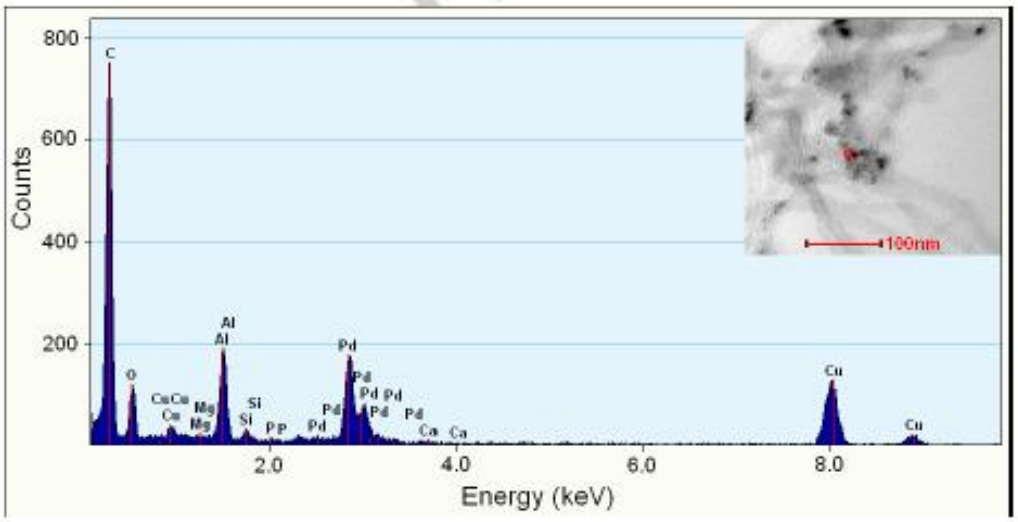

Figure 6.

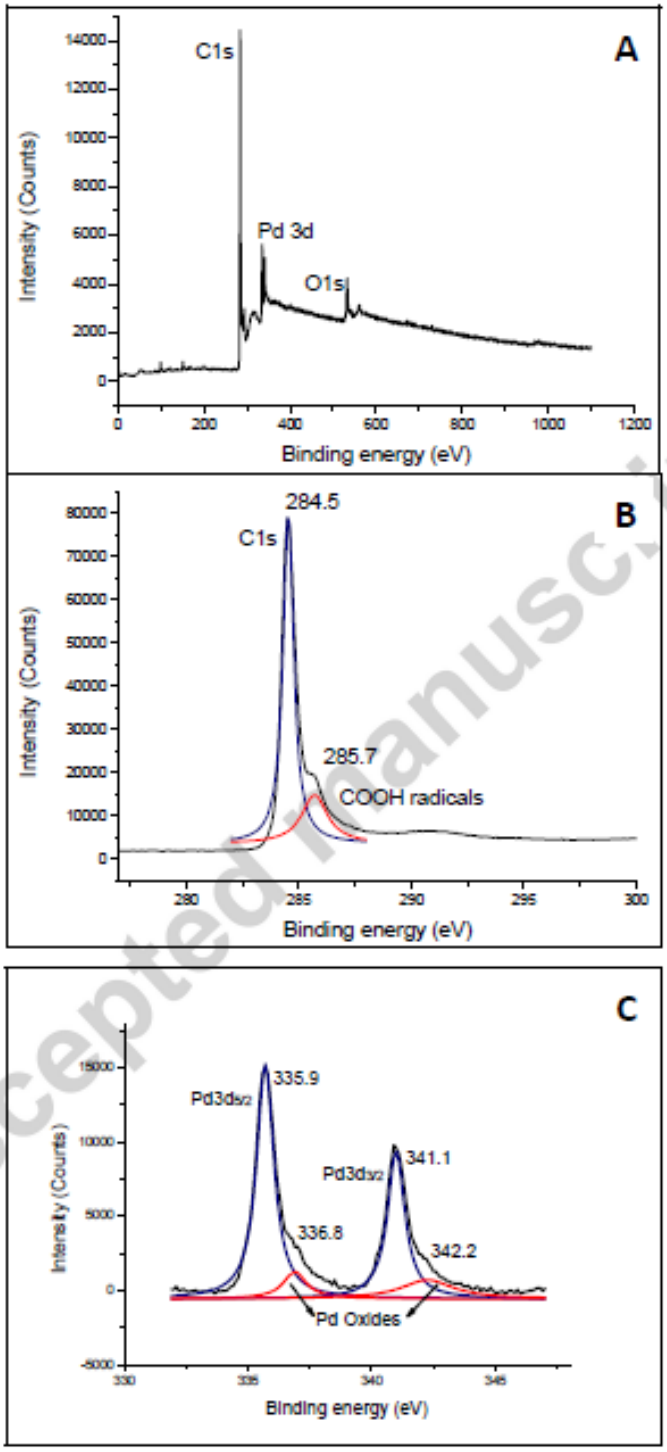

BIBLIOGRAPHY

[1] Valentin N. Popov. "Carbon nanotubes: properties and application," Materials Science and Engineering R 43, 2004, pp 61–102.

[2] Peng-Xiang Hou, Chang Liu, Hui-Ming Cheng. "Purification of carbon nanotubes," Carbon 46, 2008, pp 2003-2025.

[3] Hui-Ming Cheng, Quan-Hong Yang, Chang Liu. "Hydrogen Storage in Carbon Nanotubes," Carbon 39, 2001, pp 1447–1454.

[4] Y.L.Chen, B.Liu, J.Wu, Y.Huang, H.Jiang, K.C.Hwang. "Mechanics of hydrogen storage in carbon nanotubes," Journal of the Mechanics and Physics of Solids 56, 2008, pp 3224–3241.

[5] R.B. Rakhi, K. Sethupathi, S. Ramaprabhu, "Synthesis and hydrogen storage properties of carbon nanotubes," International Journal of Hydrogen Energy 33, 2008, pp 381 – 386.

[6] Peng-Xiang Hou, Shi-Tao Xu, Zhe Ying, Quan-Hong Yang, C. Liu, Hui-Ming Cheng. "H ydrogen adsorption / desorption behavior of multi-walled carbon nanotubes with different diameters," Carbon 41, 2003, pp 2471–2476.

[7] Arindam Sarkar, Rangan Banerjee. "A quantitative method for characterization of carbon nanotubes for hydrogen storage," International Journal of Hydrogen Energy 29, 2004, pp 1487 – 1491.

[8] Vasilios Georgakilas, Dimitrios Gournis, Vasilios Tzitzios, Lucia Pasquato, Dirk M. Guldie and Maurizio Prato. "Decorating carbon nanotubes with metal or semiconductor nanoparticles," J. Mater. Chem. 17, 2007, pp. 2679–2694.

[9] Nikolaos Karousis, Georgia-Eleni Tsotsou, Fabrizio Evangelista, Petra Rudolf, Nikitas Ragoussis, and Nikos Tagmatarchis. J. Phys. Chem. 112, 2008, pp. 13463–13469.

[10] V. Skakalova, M. Hulman, P.Fedorko, P.Lukac, S.Roth. "Effect of Gamma-Irradiation on Single-Wall Carbon Nanotube Paper," Proceedings of the IWEPNM Conference, Kirchberg, Tirol, March 8–15 (2003).

[11] Jacqueline Belloni, Mehran Mostafavi, Hynd Remita, Jean-Louis Marignier and Marie-Odile Delcourt. "Radiation-induced synthesis of mono-and multi-metallic clusters and nanocolloids," New J. Chem., 1998, pp. 1239-1255.

[12] Fu-Ken Liu, Ya-Chuan Hsu, Ming-Huei Tsai, Tieh-Chi Chu. "Using γ-irradiation to synthesize Ag nanoparticles," Radiation Physics and Chemistry, 67, 2003, pp. 517–521.

[13] Xinyun Zhang, YinYe, HengdongWang, SideYao . "Deposition of platinum–ruthenium nano-particles on multi-walled carbon nano-tubes studied by gamma-irradiation," Radiation Physics and Chemistry, 79, 2010, pp. 1058–1062.

[14] Ray H. Baughman, Anvar A. Zakhidov, Walt A. de Heer. "Carbon Nanotubes—the Route Toward Applications," Science, 297, 2002, pp 787-792.

[15] Mei Zhang and Jian Li. "Carbon nanotubes in different shapes," Materials today 12 (6), 2009, pp 12-18.

[16] T. Belin, F. Epron. "Characterization methods of carbon nanotubes: a review," Materials Science and Engineering B, 119, 2005, pp 105–118.

[17] R. Strobel, J. Garche, P.T. Moseley, L. Jorissen, G. Wolf. "Hydrogen storage by carbon materials," Journal of Power Sources 159, 2006, pp 781–801.

[18] A. Loiseau et al., Springer 2006. Understanding Carbon Nanotubes. Lect. Notes Phys. 677.

[19] Iosif Daniel Rosca, Fumio Watari, Motohiro Uo, Tsukasa Akasaka. "Oxidation of multiwalled carbon nanotubes by nitric acid," Carbon, 43, 2005, pp 3124–3131.

[20] Hui Hu, Bin Zhao, Mikhail E. Itkis, and Robert C. Haddon. "Nitric Acid Purification of Single-Walled Carbon Nanotubes," J. Phys. Chem. B, 107, 2003, pp 13838-13842

[21] Yu Li1, Xiaobin Zhang, Junhang Luo, Wanzhen Huang, Jipeng Cheng, Zhiqiang Luo, Ting Li, Fu Liu, Guoliang Xu, Xiaoxing Ke, Lin Li, and Herman J Geise. "Purification of CVD synthesized single-wall carbon nanotubes by different acid oxidation treatments," Nanotechnology, 15, 2004, pp 1645–1649.

[22] Geon-Woong Lee, Jungsoo Kim, Jinhwan Yoon, Jong-Seong Bae, Byeong Chul Shin,Il Soo Kimb, Weontae Oh, Moonhor Ree. "Structural characterization of carboxylated multi-walled carbon nanotubes," Thin Solid Films, 516, 2008, pp 5781–5784

[23] L. Stobinski, B. Lesiaka, L. Kover, J. Toth, S. Biniak, G. Trykowski, J. Judek. "Multiwall carbon nanotubes purification and oxidation by nitric acid studied by the FTIR and electron spectroscopy methods," Journal of Alloys and Compounds, 501, 2010, pp 77–84.

[24] Aiping Yu, Elena Bekyarova, Mikhail E. Itkis,Danylo Fakhrutdinov, Robert Webster, and Robert C. Haddon. "Application of Centrifugation to the Large-Scale Purification of Electric Arc-Produced Single-Walled Carbon Nanotubes," J. AM. CHEM. SOC., 128, 2006, pp 9902-9908.

[25] Andreas Hirsch. "Functionalization of Single-Walled Carbon Nanotubes, minireview," Angew. Chem. Int. Ed. 41 (11), 2002, pp 1853-1859.

[26] E. Titus, N. Ali, G. Cabral, J. Gracio, P. Ramesh Babu, and M.J. Jackson. "Chemically Functionalized Carbon Nanotubes and Their Characterization Using thermogravimetric Analysis, Fourier Transform Infrared, and Raman Spectroscopy," Journal of Materials Engineering and Performance, Volume 15 (2), 2006, pp 182-186

[27] A. V. Krasheninnikov and K. Nordlund. "Ion and electron irradiation-induced effects in nanostructured materials," Journal of applied physics, 107 (071301), 2010, 1-70

[28] Makala S. Raghuveer, Ashavani Kumar, Matthew J. Frederick, Gregory P. Louie, P. Gopal Ganesan, and Ganapathiraman Ramanath. "Site-Selective Functionalization of Carbon Nanotubes," Adv. Mater. 18, 2006, pp 547–552.

[29] V.Skakalova, U.Dettlaff-W eglikowska, S.Roth. "Gamma-irradiated and functionalized single wall nanotubes," Diamond and Related Materials 13, 2004, pp. 296–298.

[30] Martin Hulman, Viera Skákalová, Siegmar Roth Hans Kuzmany. "Raman spectroscopy of single-wall carbon nanotubes and graphite irradiated by γ rays," Journal of applied physics, 98 (024311), 2005, pp 1-6.

[31] Jinxue Guo, Yuguo Li, Shengwei Wu andWenxin Li. "The effects of γ-irradiation dose on chemical modification of multi-walled carbon nanotubes," Nanotechnology, 16, 2005, pp 2385–2388.

[32] Liangti Qu and Liming Dai. "Substrate-Enhanced Electroless Deposition of Metal Nanoparticles on Carbon Nanotubes," J. AM. CHEM. SOC. 127, 2005, pp 10806-10807

[33] Bin Xue, Ping Chen, Qi Hong, Jianyi Lin and Kuang Lee Tan. "Growth of Pd, Pt, Ag and Au nanoparticles on carbon nanotubes," J. Mater. Chem. 11, 2001, pp 2378-2381.

[34] Zhenyu Sun, Zhimin Liu, Buxing Han, Shiding Miao, Zhenjiang Miao, Guimin An. "Decoration carbon nanotubes with Pd and Ru nanocrystals via an inorganic reaction route in supercritical carbon dioxide–methanol solution," Journal of Colloid and Interface Science, 304, 2006, pp 323–328.

[35] Seong-Dae Oh, Bong-Keun So, Seong-Ho Choi, A. Gopalan, Kwang-Pill Lee, Kuk Ro Yoon, Insung S. Choi. "Dispersing of Ag, Pd, and Pt–Ru alloy nanoparticles on single-walled carbon nanotubes by g-irradiation," Materials Letters, 2005, 59, 2005 pp 1121–1124.

[36] Mélanie Spotheim-Maurizot, Mehran Mostafavi, Jacqueline Belloni, Thierry Douki. Radiation chemistry: From basics o applications in material and life science, chapter 7. EDP Sciences, 2008

[37] I.P. Jain. "Hydrogen the fuel for 21st century," International journal of hydrogen energy, 34, 2009, pp 7368–7378

[38] Yuda Yuruma, Alpay Taralp, T. Nejat Veziroglu. "Review Storage of hydrogen in nanostructured carbon materials," International journal of hydrogen energy, 3 4, 2009, pp 3784–3798.

[39] M. Hirscher, M. Becher, M. Haluska, A. Quintel, V. Skakalova, Y.-M. Choi, U. Dettlaff-Weglikowska , S. Roth , I. Stepanek , P. Bernier, A. Leonhardt , J. Fink. "Hydrogen storage in carbon nanostructures," Journal of Alloys and Compounds, 330–332, 2002, pp 654–658.

[40] H. Takagi, Y. Soneda, H. Hatori, Z.H. Zhu, and G.Q. Lu. Hydrogen adsorption properties of single-walled carbon nanotubes treated with nitric acid. ICONN 2006.

[41] A.M. Rashidi, A. Nouralishahi , A.A. Khodadadi, Y. Mortazavi, A. Karimi, K. Kashefi. "Modification of single wall carbon nanotubes (SWNT) for hydrogen storage," International journal o f hydrogen energy, 35, 2010, pp 9489-9495.

[42] Renju Zacharia, Keun Young Kim, A.K.M. Fazle Kibria, Kee Suk Nahm. "Enhancement of hydrogen storage capacity of carbon nanotubes via spill-over from vanadium and palladium nanoparticles," Chemical Physics Letters, 412, 2005, pp369–375.

[43] Y. Suttisawat, P. Rangsunvigit, B. Kitiyanan, M. Williams, P. Ndungu, M.V. Lototskyy, A. Nechaev, V. Linkov, S. Kulprathipanja. "Investigation of hydrogen storage capacity of multi-walled carbon nanotubes deposited with Pd or V," International journal of hydrogen energy, 34, 2009, pp 6669–6675.

[44] Rather, Sami-ullah, Zacharia, Renju, Hwang, Sang Woon, Naik, Mehraj-uddin, and Nahm, Kee Suk, "Hydrogen uptake of palladium embedded MWCNTs produced by impregnation and condensed phase reduction method," Chemical Physics Letters, 441(4-6), 2007, pp 261-267.

[45] Mu, Shi-chun, Tang, Hao-lin, Qian, Shen-hao, Pan, Mu, and Yuan, Run-zhang, "Hydrogen storage in carbon nanotubes modified by microwave plasma etching and Pd decoration," Carbon, 44(4), 2006, pp 762-767.

[46] S. Goyanes, G.R. Rubiolo, A. Salazar, A. Jimeno, M.A. Corcuera, I. Mondragon. "Carboxylation treatment of multiwalled carbon nanotubes monitored by infrared and ultraviolet spectroscopies and scanning probe microscopy," Diamond & Related Materials, 16, 2007, pp 412–417.

[47] A. Appleby, Harold A. Schwarz. "Radical and molecular yields in water irradiated by .gamma.-rays and heavy ions," J. Phys. Chem., 1969, 73 (6), pp 1937–1941

[48] Michaelis, M., Henglein, "A. Reduction of Pd(II) in Aqueous Solution: Stabilization and Reactions of an Intermediate Cluster and Pd Colloid Formation," J. Phys. Chem. 96, 1992, pp 4719-4724.

[49] Hynd Remita, Samy remita. Metal cluster and Nanomaterials. Contribution or radiation chemistry. Recent trends in radiation chemistry pp 347-383.

[50] A. Sarkany, Z. Papp, I. Sajo, Z. Schay. "Unsupported Pd nanoparticles prepared by gamma-radiolysis of $PdCl_2$," Solid State Ionics 176, 2005, pp 209–215.

[51] L. Vaisman, H. D. Wagner, G. Maroma. "The role of surfactants in dispersion of carbon nanotubes," Advances in Colloid and Interface Science, 2006, 128–130, pp 37–46

[52] J. Rojas, C. H. Castano. "Production and characterization of supported transition metal nano-particles on multi-walled carbon nanotubes functionalized by gamma irradiation and chemical processes." Supplemental proceedings: volume 1: materials processing and energy materials TMS (the minerals, metals & materials society), 2011

[53] Charles D. Wagner, Alexander V. Naumkin,Anna Kraut-Vass, Juanita W. Allison, Cedric J. Powell, and John R. Rumble, Jr.NIST Standard Reference Database 20, Version 3.5.

VITA

Jessika Viviana Rojas Marin was born in Medellin, Colombia. She was accepted into the Physics School at the National University of Colombia in 2001 and graduated in July 2006 with a Bachelors of Science in Engineering Physics. During her undergraduate, Jessika was a member of the Radiology group where she developed her thesis entitled "Dose quantification in mammography studies". A year after graduation, Jessika started a master in the School of Materials Engineering at the same University, and became a member of the Tribology and Surfaces group (GTS). Her research was focus on the identification and quantification of phases of ASTM A743 grade CA6NM cast martensitic stainless steel through high-temperature x-ray diffraction. Jessika graduated in 2009 with a Master in Engineering- Materials and processes.

She then pursued a second Master degree in Nuclear Engineering at the Missouri University of Science and Technology, which was awarded in December 2011.